PROBING CONVERGENCE IN ORTHOGONAL CONJUGATED POLYMER CATALYSIS BY T4 LYSOZYME UTILIZING BIOPHYSICAL CHARACTERIZATION

by

William D. Turner

Bachelor of Science (B.S.) in Biochemistry

Kennesaw State University, 2020

Thomas C. Leeper Laboratory

Submitted in partial fulfillment of the requirements

For the Degree of Master of Science in Chemical Sciences in the

Department of Chemistry and Biochemistry

Kennesaw State University

2022

---	---
Committee Chair	Graduate Program Coordinator
---	---
Committee Member	Department Chair
---	---
Committee Member	College Dean

ACKNOWLEDGEMENTS

One page. This page. To thank you all, for whom believed in me.

I would like to start by thanking my PI, Dr. Thomas C. Leeper. Your mentorship, encouragement, countless scenarios to make me delve deeper into the science *(whilst not burying the lede)*, and overall patience these last four years… I can never thank you enough or tell you how appreciative I am for all you have taught me and I hope I have made you proud. I would also like to thank both of my committee members, Dr. Susan M.E. Smith and Dr. Jonathan L. McMurry; your combined force of direction, advice, and pushing me in the right direction truly made this experience worthwhile. From the start, all three of you promised to not let up or go easy on me, a daunting task to say the least. I thank you all for challenging me and imparting the skills and mindset necessary to achieve my future career aspirations. I can say I am truly the better for it.

My lab mates — though many have come and gone over the years — to say I'm grateful for your presence in my life would be an understatement. My fellow Leeper Lab colleagues, you will never know how indebted I am to each of you; you truly made the difference in those moments I doubted myself. To Katherine Letsinger: your wit, knowledge, and continuous banter kept me motivated and driven right down to the midnight hour. To Conner Casterline — though you were prone to dozing off, you always made time to listen and offer a hug when I needed it. To Amani Gaddy — your peace of mind and quips of sarcasm were exactly what was needed during those difficult and trying days as we neared the final stretch. And of course, to Sarah Waldron — from your considerable patience during those early research days, to the tears shared on the very last, your knowledge, encouragement, and unwavering friendship over the years is something I could never thank you enough for. This EGG did good.

Amongst the colleagues and lifelong friends standing beside me at the finish line, I can not go without thanking my family, namely my mother and father, Cynthia and Derrick Turner. From a young age, they instilled both a passion for learning and the pursuit of achieving one's' dreams and how both do not come without sacrifice and perseverance.

Though last, Kennesaw State University has been a pinnacle in my academic career and has certainly transformed me into the scholar and scientist I have become. Through the many credits, the generous graduate funding, the teaching opportunities, and — above all — the many faculty members who I've had the pleasure to learn from, your continuous support and encouragement were pivotal in the completion of my journey at this institution. This work and the decade spent here is truly a coming of age… and it's because of you all that I made it.

ABSTRACT

Conjugated polymers have become highly attractive as they afford unique material properties that make them promising for a wide range of applications, such as photovoltaics and drug delivery systems. However, these conjugated polymers require extensive synthetic steps involving hazardous organic solvents or metal-based catalysts yielding toxic waste streams. To remedy this, enzymes have emerged as a highly valuable alternative to synthesizing these polymers as they are able to be produced in environmentally benign conditions and have played a pivotal role in various biosynthetic strategies in recent years.

Serving as model systems, lysozymes have been shown to polymerize 2-ethynylpyridine (2-EP) via orthogonal catalysis to produce a conjugated polymer with pyridine pendant groups. Initial studies utilized hen egg-white lysozyme (HEWL), however, the deduction of its mechanism was limited since tools for modifying the protein for detailed studies of structure activity relationships were intractable. In this work, bacteriophage T4 lysozyme (T4L) has been adapted to polymerize 2-EP and has been investigated using various biophysical methods to probe the convergence between glycosidic hydrolase classes in their ability to produce this conjugated polymer. Though the polymerization mechanism remains elusive, this initial work suggests these systems may be adaptable for ‘green’ approaches in emerging materials technology and biomedical facets.

TABLE OF CONTENTS

LIST OF ABBREVIATIONS

Å	Angstrom
^{o}C	Degrees in Celsius
ΔH	Enthalpy Change
ΔS	Entropy Change
λ	Wavelength
µg	Microgram
µL	Microliter
µM	Micromolar
% w/v	Percent Weight per Volume
2-EP	2-ethynylpyridine
2X-YT	2x Yeast Extract and Tryptone
Abs	Absorbance
AU	Absorbance Units
BLI	Biolayer Interferometry
CM	Carboxymethyl
CSPs	Chemical Shift Perturbations
D_2O	Deuterium Oxide
DI	Deionized
DMSO	Dimethyl Sulfoxide
DPP	1,3-di(2-pridyl)propane
EDTA	Ethylenediaminetetraacetic acid
FF	Fast Flow

F.W.	Formula Weight
g	Gram
GPC	Gel Permeation Chromatography
HEDS	2-Hydroxyethyl Disulfide
HEWL	Hen Egg-white Lysozyme
Hrs.	Hours
HSQC	Heteronuclear Single Quantum Coherence
IEX	Ion Exchange Chromatography
IMAC	Immobilized Metal-Ion Affinity Chromatography
ITC	Isothermal Titration Calorimetry
J	Joule
K	Kelvin
K_D	Dissociation Constant
kDa	Kilodalton
kJ	Kilojoule
L	Liter
LB	Luria Broth
M	Molar
MΩ	Mega Ohm
M9	Minimal Media
mAU	Milli Absorbance Units
mg	Milligram
MHz	Megahertz

min	minute
mL	Milliliter
mol	Mole
mm	Millimeter
mM	Millimolar
mV	Millivolt
n	Numerical Value of Ligand
^{15}N	Isotopically Labelled Nitrogen
NAG	*N*-acetylglucosamine
$(NAG)_3$	N,N′,N″-Triacetylchitotriose
NAM	*N*-acetylmuramic acid
NBP	Non-binding Proteins
NEB	New England Biolabs
ng	Nanogram
NHS-LC-LC	Sulfosuccinimidyl-6-[biotinamido]-6-hexanamido Hexanoate
nm	Nanometer
NMR	Nuclear Magnetic Resonance
O.D.	Optical Density
OLED	Organic Light-Emitting Diode
paIVY	*Pseudomonas aeruginosa* Inhibitor of Vertebrate Lysozyme
PBS	Phosphate Buffered Saline
PCR	Polymerase Chain Reaction
PDB	Protein Data Bank

PEG	Polyethylene Glycol
pH	Hydrogen Ion Concentration
pI	Isoelectric Point
PDVF	Polyvinylidene Fluoride
R^2	Correlation Coefficient
rpm	Rotations Per Minute
s	Seconds
SARs	Structure-activity Relationships
SDM	Site-directed Mutagenesis
SDS	Sodium Dodecyl Sulfate
SEC	Size Exclusion Chromatography
SP	Sulphopropyl
STD	Saturation Transfer Difference
T_0	Initial Starting Point Within a System
T4L	Bacteriophage T4 Lysozyme
TBS-T	Tris Buffered Saline with Tween-20
TEV	Tobacco Etch Virus
TROSY	Transverse Relaxation Optimized Spectroscopy
V	Volt
WT*	Wild-Type Null of Cysteine Residues
XRC	X-Ray Crystallography

LIST OF FIGURES

LIST OF EQUATIONS

CHAPTER I – INTRODUCTION

1.1 Conjugated Polymers and Their Various Applications

In an era of medical and scientific advancement, conjugated polymers have attracted significant attention in the production of renewable energy sources; this is in part due to the tunability of their molecular structures making them suitable for a wide range of specific applications.[1, 2] Of these, organic light-emitting diodes (OLEDs) are of considerable interest as numerous conjugated polymers have been studied due to their semiconductive nature and provide an array of potential routes for recyclable energy and reduced waste in material development.[3]

Similarly, biomedical applications have also evoked the utilization of conjugated polymers by adapting such to various procedures and stratagems in medical imaging, one of which involving the use of nanoparticles – the benefit being such particles are able to be applied in the staining of cells or tissue for techniques, such as microscopy and tomography,[4] whilst affording low cytotoxicity for the patient. Further applications in this field have shown polymers being exploited for the manifestation of biosensors in instrumentation for various genetic testing and medical diagnostics. [6]

1.2 Challenges and Implications from Traditional Organic Synthesis

Though these polymers have established utility in several fields and have undergone substantial studies of mechanisms, their syntheses often require the use of organic solvents and metal-containing catalysts that result in the production of toxic

byproducts, such as halogenated organic compounds or undesired metal complexes. (Figure 1)

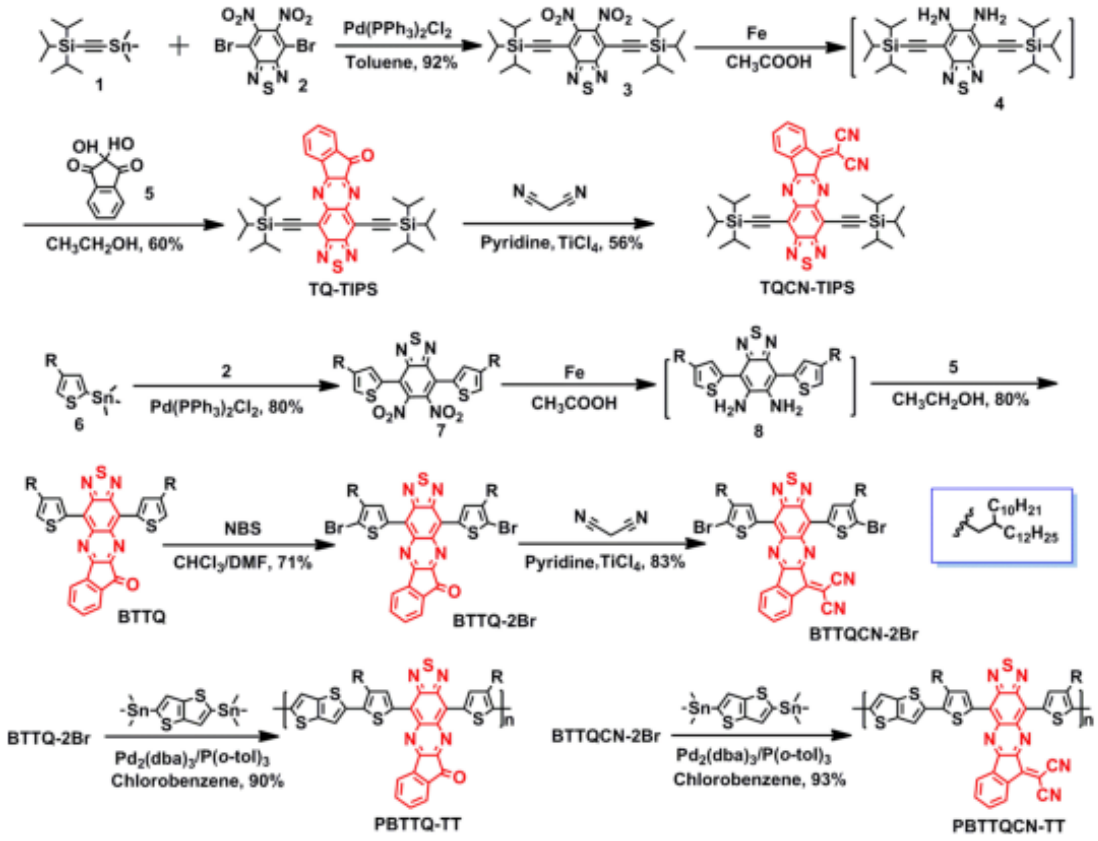

Figure 1. Scheme depicting traditional syntheses necessary in the production of a conjugated polymers. Most polymer creation undergoes extensive multistep synthesis and require harmful reagents.[5]

These types of traditional organic syntheses often utilized in the creation of conjugated polymers – aside from oxidation or radial polymerizations – can be classified as either Grignard metathesis or palladium catalyst pathways. [7,8]

Grignard metathesis schemes involve the intercalation between polythiophene compounds and through a repetitive oxidative initiation, transmetalation propagation, and reductive elimination mechanism produce the conjugated polymer;[8] however, due to the

nature of their respective atoms, polythiophenes are highly pyrophoric and institute an array of hazardous conditions for the chemist. Similar strategies perform polycondensation reactions via palladium catalysts to produce conjugated polyaromatics which play a pivotal role in emerging materials technology.[7,8] Albeit some of these polycondensations involve highly toxic reactants in their mechanisms, such as tin, which present both potential environmental and health implications.

1.3 "Greener" Routes Afforded via Enzymes

To address this problem, enzymes have been proposed as viable substitutes in these processes, as they have been a staple in various biosynthetic strategies;[9,10] more so, specificity and selectivity suggest that enzymes may be more advantageous than that of traditional small molecule catalysts. Enzymes provide additional advantages in that they are active in water and can be derived from renewable sources, eliminating the need for extensive syntheses involving organic solvents. While enzymes have adapted to some polymerization reactions, not all have been extensively explored in the production of conjugated polymers;[11,13] however, a subclass of enzymes may be tailored into the development of sustainable routes for "greener polymer chemistry." The work described herein pertains to the adaptation of existing glycoside hydrolase enzymes for enzymatic synthesis of a conjugated polymer.

Lysozymes – often referenced as muramidases – are enzymes that play a vital role in the innate immune system as they contribute to the breakdown of peptidoglycan linkages found in gram-positive bacteria;[14] this degradation is catalyzed via the hydrolysis of the β-1,4 glycosidic linkages found between the *N*-acetylglucosamine (NAG) and *N*-

acetylmuramic acid (NAM) subunits. (Figure 2) As these enzymes are found across many taxa, they afford a variety of avenues in development of conjugated polymers.

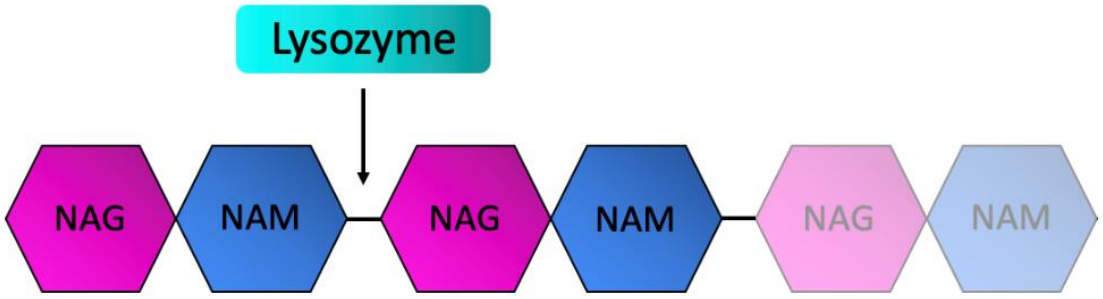

Figure 2. Composition of peptidoglycan subunits and lysozyme's role. Repeating subunits, *N*-aceytlglucosamine (NAG) and *N*-acetylmuramic acid (NAM), that comprise the peptidoglycan found in gram-positive bacteria. B-1,4 linkage being cleaved via lysozyme. Figure adapted from Irazoki et al.[12]

1.3.1 Hen Egg-white Lysozyme (HEWL)

Of these, hen egg-white lysozyme (HEWL) is one of the most highly characterized proteins as its structure activity relationships (SARs) have been investigated for several decades. This lysozyme is a monomeric 129-residue protein with a molecular weight of approximately 14.5 kDa and its native structure was first determined using X-ray crystallography [15] and was one of the first proteins to be investigated using NMR spectroscopy. [17,18] It consists of two domains: an α- domain (residues 1-35 and 85-129), comprised of four α-helices and a β-domain (residues 36-84) containing a triple-stranded anti-parallel β-sheet and a dynamic loop region. (Figure 3a) As this lysozyme has been extensively characterized, HEWL serves as a model system in the investigation of enzymes influencing conjugated polymer formation.

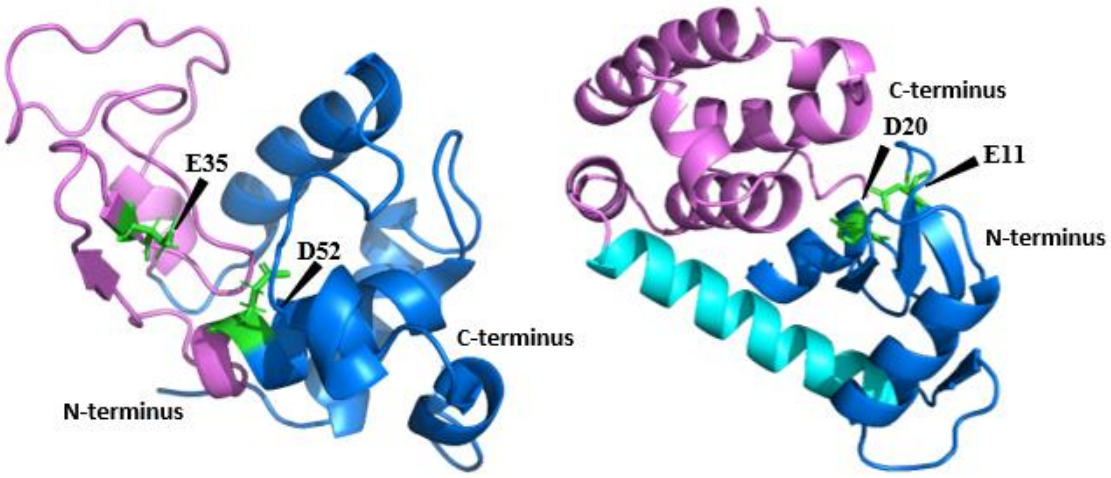

Figure 3. Structural comparison between hen egg white lysozyme (PDB: 1E8L) (a) and bacteriophage T4 lysozyme (PDB: 2LZM) (b). Catalytic residues known to either lysozyme have been denoted in green. α – and β-domains for each protein are colored purple and blue, respectively. α-helix bridging domains in T4L can be seen in cyan. Image produced via PyMOL software.

Previous studies have shown, in the presence of HEWL, 2-ethynylpyridine (2-EP) produces a conjugated pyridine-pendant polymer with a strong red hue without the use of organic solvents or metal-based catalysts. Further characterization revealed unusual kinetic properties, observing a sigmoidal curve, often seen with cooperatively allosteric enzymes, with increasing substrate concentration of 2-EP. (Appendix A.1) Additionally, trials to obtain HEWL complexed with 2-EP was obtained using crystallography that provided diffraction data necessary in identifying how substrate is recognized within this system – this is later presented in Chapter V.

Although these data were promising, limitations came when attempting to understand other aspects afforded by this lysozyme. HEWL is relatively inexpensive and is readily commercially available. However, since it is derived from a nature source, its

sequence cannot be easily manipulated to assess which residues support polymerization. Furthermore, by isotopically labelling the protein we can utilize NMR to analyze changes in the chemical environment brought about from the incorporation of 2-EP monomer; most strategies for isotopic labeling require that the protein is produced from engineered heterologous expression systems. Therefore, other sequences were examined to identify a glycoside hydrolase with similar sequence identity but that was amenable to expression in *E. coli* to allow for these additional experiments to be conducted.

1.3.2 Bacteriophage T4 Lysozyme (T4L)

In comparison to HEWL, bacteriophage T4 lysozyme (T4L) exhibits similar characteristics that serve as a viable construct in probing variable aspects affording mechanistic determination. (Figure 3b) Striking similarities can be visualized between lysozymes, as both have a bi-lobal conformation and have similar molecular weights and amino acid sequences – T4L is a monomeric 164-residue protein approximately 18.7 kDa. Of more interest, literature provides evidence identifying a correspondence of 78 residues between the lysozymes three-dimensional structures; [16] furthermore, the active site residues of both HEWL and T4L are also conserved, E35/D52 and E11/D20, respectively. The combination of these similarities suggests the two lysozymes may have evolved from a common precursor. (Figure 4)

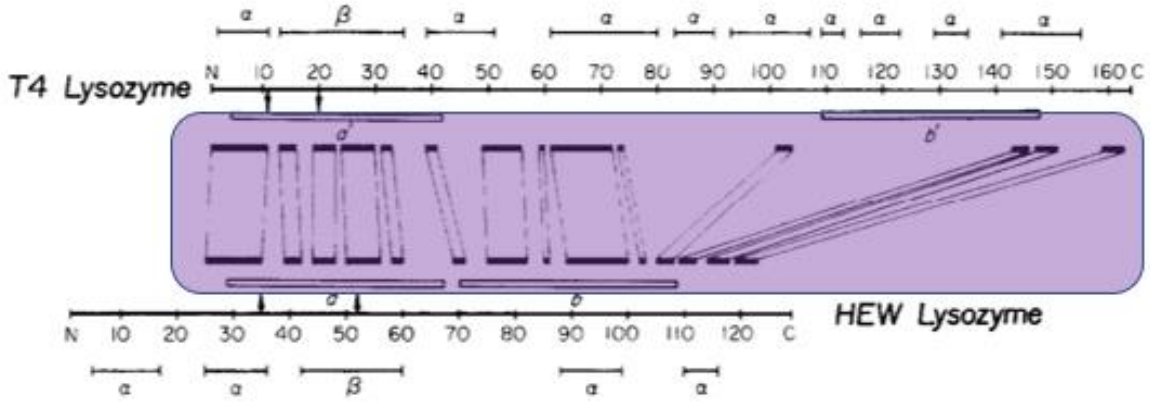

Figure 4. Schematic diagram showing the relation between the backbones of bacteriophage T4 lysozyme (T4L) and hen egg white lysozyme (HEWL). Shaded purple region highlights stretches indicating the equivalent residues per the alignment. Figure adapted from Rosemann and Arpos.[16]

1.4 Research Motivation and Aims

The intent of this research was to determine if another glycosidic hydrolase, such as T4L, could perform similar orthogonal catalysis as well as attempt to elucidate the mechanism that is use for the interaction between lysozyme and 2-EP. To achieve this, molecular subcloning was performed on the original T4L construct incorporating a different purification method to overcome initial low protein yields. Site-directed mutagenesis was conducted to probe how changing the active sites of this lysozyme compromises its inherent function and rate of polymer accumulation – these will be assessed using various assays later discussed.

Comparative analysis relied on further characterization strategies using various biophysical techniques; their intent was to assess other attributes unique to each variant, such as: proper protein folding and interaction between protein and enzyme, determination of binding affinities, and assessment of both the thermodynamic and

stoichiometric properties. In addition, crystallography was attempted to produce a protein-enzyme complex that can provide insight into how the 2-EP substrate is recognized by these lysozymes using electron density mapping and diffraction data.

CHAPTER II – T4 LYSOZYME EXPRESSION AND PURIFICATION STRATEGIES *IN TANDEM* WITH SITE-DIRECTED MUTAGENESIS

2.1 Introduction

Biochemistry laboratories depend upon ready access to purified protein when performing various kinetic and characterization studies. Although protein can be purchased from commercial sources, traditional routes rely on in-house production via bacterial expression followed by a purification strategy unique to the protein vector, typically involving a series of chromatography steps. Relevant to this project, the initial T4L construct expressed protein that used an established but an impractical protocol requiring a pair of lengthy ion-exchange purification steps. The following sections describe an initial ion-exchange-based T4L purification strategy developed by Matthews and colleagues,[19] that was used in initial studies related to this work, and subsequent modifications to that procedure to develop a refined protocol that takes advantage of the introduction of a fusion tag to enhance the quality, quantity, and rapidity of T4L purification to support structural and biophysical studies.

Ion-exchange chromatography (IEX) is a purification strategy that separates biomolecules based on differences in their net surface charge; as molecules vary in their charge properties, each exhibits different degrees of interaction when in the presence of charged, chromatography media.[20] Due to the ionizable groups present on these molecules, their net surface charge can be impacted by varying pH, that is, they are highly pH dependent. IEX takes advantage of this relationship, in purifying proteins, by

varying the binding favorability of specific molecules using buffers with pH values either above or below the isoelectric point (pI) of the protein.[21] The protein undergoes a dual ion-exchange purification – first using a weak cation system (CM Sepharose) followed by a strong cation system (SP Sepharose) – and is refined further using size-exclusion chromatography (SEC) to limit potential impurities or protein oligomerization.

Although a purification protocol for T4L exists using the above strategy, IEX comes with limitations preventing the further characterization studies necessary in determining this elusive polymer-protein mechanism. Of these, obtaining sufficient protein proved the most difficult; with consistent yields estimating 12 mg of purified protein from a 2-liter bacterial culture, a different purification construct was suggested. By excising the T4L sequence from the initial vector and subcloning into another that employs a poly-histidine tag followed by a cleavage site, immobilized ion-metal affinity chromatography (IMAC) was suggested to not only be a more efficient strategy but to optimize the eventual yield of the protein.

Contrary to ion-exchange, IMAC separates proteins in accordance with their affinity for metal ions that have been immobilized by chelation to an insoluble matrix;[22] of the transition metals, cobalt and nickel have been shown to be the most effective.[23] Proteins involved in IMAC incorporate a poly-histidine tag, as histidine's imidazole ring serves as a high-affinity binder to the metal ions present; this interaction allows for residual debris and nonspecific binding protein (NBP) removal leading to a degree of purity of the target protein. A modified strategy is used within the Leeper Laboratory – commonly referenced as a 'cleave-and-clear' method – which inserts a cleavage sequence [ENLYFQ | G/S] following said tag to be later cleaved via Tobacco Etch virus (TEV)

protease and cleared by a secondary, IMAC purification. Like IEX, a subsequent SEC step removes additional protein impurities, oligomers, and aggregates.

Site-directed mutagenesis (SDM) was later initiated to probe for mechanistic determination. Stated in Chapter I, numerous studies in the literature show conservation of amino acid residues within a family of proteins may contribute to either the structural integrity of the protein, play a vital role in catalysis, or both.[24] With the incorporation of mutations, each variant may provide insight into what aspect of the protein attributes to the formation of the conjugated polymer, poly-2-EP.

2.2 Experimental Design

2.2.1 Molecular Subcloning Design

The pBAD His/A vector was purchased from Invitrogen (Fisher Scientific, Waltham, MA) and subcloned using plasmid cloning via restriction enzyme digest protocol provided by Addgene.[40] Restriction digests were performed on both donor and recipient plasmids using 1µL of New England Biolabs enzymes NcoI and HindIII in CutSmart buffer at 37°C for 1 hour. The reaction was loaded into an agarose gel and subjected to 100 V for 45 minutes; bands indicative of T4L insert and cut pBAD His/A vector were excised and purified using QC solubilization buffer (Qiagen, Hilden, Germany). Purified insert and vector product concentrations were 71 ng/μL and 83 ng/μL, respectively.

DNA ligation was conducted following gel purification; reactions were prepared using a 3:1 ratio of insert to vector (3.5 μL: 1 μL), 1 μL of 10x ligase buffer, 1 μL of T4 DNA ligase, totaled to a volume of 10 μL using nuclease-free water, and run overnight at 16° per manufacturer's protocol.[41] The resulting ligation reaction was transformed into *E.*

coli DH5–α and following standard procedures; bacteria were plated on LB agar plates enriched with 50 µL of ampicillin and incubated at 37°C overnight. Single, isolated colonies were grown in overnight cultures of 15 mL LB media in preparation for mini-prep. Cells were harvested and mini-prepped using the E.Z.N.A. Plasmid DNA Mini Kit II (Omega Bio-Tek, Norcross, GA) protocol. Plasmid concentrations were determined using a nanodrop and later sequence validated via Genewiz Sanger sequencing.

2.2.2 Protein Expression and IMAC Purification

Subcloned T4L-10xHIS protein was prepared using competent *E. coli* BL21-(DE3) pLysS and grown at 37°C overnight on LB agar plates enriched with ampicillin. Of the transformed colonies, 2-3 colonies were sterilely looped into two 50 mL cultures of 2X-YT media and incubated at 37°C overnight. These small volume cultures were divided into 2 Fernbach flasks containing ^{15}N M9 minimal media and further incubated at 37°C until the culture reached an optical density (OD_{600}) of 0.4-0.6; temperature of cell growth was reduced to 18°C and 0.1% (w/v) of L-(+)-arabinose was added to induce protein expression overnight. Cells were harvested by centrifugation at 10,000 rpm for 10 minutes at 4°C and either lysed, as described next, or frozen at -20°C for future purifications.

Each pellet was resuspended in equilibration buffer (20 mM potassium phosphate, 200 mM potassium chloride, 20 mM imidazole, pH: 8.0) with a Pierce™ protease inhibitor tablet (Fisher Scientific, St. Louis, MO), homogenized using a Pyrex® culture grinder (ThomasFisher Scientific, Swedesboro, NJ), and then lysed using a microfluidizer chilled with ice. Lysate was centrifuged at 27,000 rpm for 45 minutes followed by the collection of the supernatant, also referred to as the crude lysate. The supernatant was

loaded by direct injection and purified using IMAC via a HisTrap FF Crude nickel-charged column (Cytiva, Marlborough, MA) affixed to an NGC chromatography system (Bio-Rad, Hercules, CA). Equilibration buffer was passed over the column until a baseline was established to ensure any impurities, such as non-binders, were no longer eluting. Following this, elution buffer (20 mM potassium phosphate, 200 mM potassium chloride, 400 mM imidazole, pH: 8.0) was passed to conduct an intermediate step-wash at 20% elution buffer to remove contaminants or NBPs followed by a continuous concentration gradient from 20% to 100% spanning 25 mL at 5 mL/min to elute the protein immobilized on the column. To chelate any residual nickel ions released during the IMAC purification, 0.5 M disodium ethylenediaminetetraacetic acid (EDTA) was added to elution peak fractions to a concentration of 500 µM and dialyzed against 20 mM potassium phosphate, 200 mM potassium chloride, pH: 8.0 using ThermoScientific SnakeSkin dialysis tubing for 4 hours at room temperature. The fractions were removed from the dialysis and 2 mg of on-site prepared TEV protease was added prior to an extended dialysis overnight. Following cleavage, a secondary IMAC purification was implemented to remove the poly-histidine tag and his-tagged TEV enzyme using the same buffer strategy as before. Fractions collected from the flow-through were concentrated to a desirable volume of 2 mL using an Amicon ultrafiltration cell (Millipore Sigma, Burlington, MA) through a 5 kDa filter. The concentrated protein was then loaded onto a HiLoad Superdex 16/600 SEC column (Cytiva, Marlborough, MA) to achieve optimal purity; the protein was loaded via direct inject against SEC buffer (filtered, 18 MΩ H_2O, pH: 7.0). Peak fractions were collected and concentrated to desired concentrations for future experiments. Purifications found a standard, two-liter prep

yielded approximately 2-4 mL of purified T4L within a concentration range of 900 μM-1.6 mM (approx.17-30 mg of purified protein per 2-liter bacterial culture).

2.2.3 Coomassie staining and Western blotting

During each step of the purification protocol, 20 µL samples were collected and diluted 1:1 with Bio-Rad 2x SDS-PAGE loading buffer (Bio-Rad, Hercules, CA) with β-2-mercaptoethanol (BME). The samples were boiled to denature the protein prior to being loaded into wells for gel electrophoresis. Two gels were electrophoresed at 200 V for approximately 40 minutes. One gel was stained using Coomassie Blue (Bio-Rad, Hercules, CA) per manufacturer protocol and imaged using a Li-Cor Odyssey system (Li-Cor, Lincoln, NE) equipped with Image Studio 5.1; the latter was prepared for western blotting.

Monoclonal anti-poly-histidine (anti-His) antibody raised in mouse (Sigma-Aldrich, St. Louis, MO) served as the primary antibody against the poly-histidine tag present in purified T4L; this was supplied at 0.5µg/µL. Secondary antibody anti-mouse raised in goat (IRDye 800CW, Li-Cor, Lincoln, NE) served to screen for primary, anti-His antibody; this was supplied at 1mg/mL.

In preparation for western blotting, the second gel along with two pieces of extra-thick (2.4 mm) filter paper were equilibrated in Towbin transfer buffer (25 mM Tris-Base, 192 mM Glycine, 20% methanol, pH: 8.3) for 10 minutes. In addition, a polyvinylidene fluoride (PVDF) transfer membrane was prepared using a serial equilibration using methanol, followed by deionized water, and then Towbin transfer buffer. Upon component assembly, proteins from the gel matrix were transferred onto the PVDF membrane for 30 minutes at 25 mV using a Bio-Rad Trans-Blot Turbo Transfer

System (Bio-Rad, Hercules, CA) and later incubated overnight at 4°C in primary anti-His α antibody – diluted 1:5000 in 12 mL Odyssey blocking buffer (Li-Cor, Lincoln, NE) and supplemented with 12 μL Tween-20 (Fisher Scientific, Waltham, MA) and 12 μL 10% SDS (Fisher Scientific, Waltman, MA)– to screen for his-tagged T4L. Following this, the primary antibody was removed, and the membrane was washed using 1x Tris buffered saline (50 mM Tris-Base, 150 mM sodium chloride, pH: 7.5) supplemented with 0.1% Tween-20. The membranes were then incubated with secondary, goat anti-mouse antibodies for one hour at room temperature, followed by a subsequent wash step using 1x TBS-T. The western blot was imaged as above.

2.2.4 Site-directed Mutagenesis Primer Design

Mutagenic primers were designed following the QuikChange site-directed mutagenesis protocol via Stratagene using PrimerX Bioinformatics software.[42] Mutating off the wild-type template, variants were incorporated by integrating a single nucleotide change. Default parameters were adjusted to provide optimal primer pairs; these were later validated using OligoCalc, checking against potential hairpins, self-annealing sites, and 3' complementarity. Each primer pair were ordered through idtDNA and arrived in a lyophilized state. Following the pfuUltra High-Fidelity DNA polymerase AD protocol, each mutation was prepared for linear amplification in tandem with negative controls. DpN1 digests were initiated following the PCR and later analyzed via agarose gel analysis.

Successful mutagenic plasmids were transformed and prepared following the mini-prep protocol detailed in 2.2.1. Plasmid concentrations were determined using a nanodrop and later sequence validated via Genewiz Sanger sequencing. Mutagenic

plasmid concentrations for E11Q and D20A were 182 ng/μL and 173 ng/μL, respectively.

2.3 Results and Discussion

2.3.1 Rationale for T4 Lysozyme Mutations

In comparing various glycosidic hydrolases, the lysozyme superfamily shares not only a common globular domain fold but maintains a β-hairpin structural motif that exhibits a strong amino acid conservation score across their aligned sequences.[16] As this motif lies adjacent to their substrate binding cleft, this conservation of residues may afford valuable insight into the variable, intrinsic properties these lysozymes may contribute to, such as catalytic mechanisms. Of the notable residues, glutamic (Glu) and aspartic acid (Asp) are of the most prevalent; both of which are conserved within the HEWL and T4L sequences – E35/D52 and E11/D20, respectively. Although both lysozymes are highly characterized and structurally determined, the role in which these residues contribute to conjugated polymer catalysis has yet to be understood. Literature suggests, of these catalytic sites located on either side of the bi-lobal interface, the glutamic acid (E) residue contributes to these lysozyme's lytic ability whereas the source for catalytic capacity resides with either the aspartic acid (D) residue or other noteworthy residues, such as T26 in T4L.[24]

In deciding which mutations to incorporate for probing studies, the notion to institute a slight variation in one active locale whist compromising the other entirely would provide valuable insight in how modest changes differ in protein functionality compared to that of greater modifications; thus, mutagenic plasmids E11Q and D20A

were created. (Figure 5) These mutations were later confirmed via commercial sequencing prior to purification attempts.

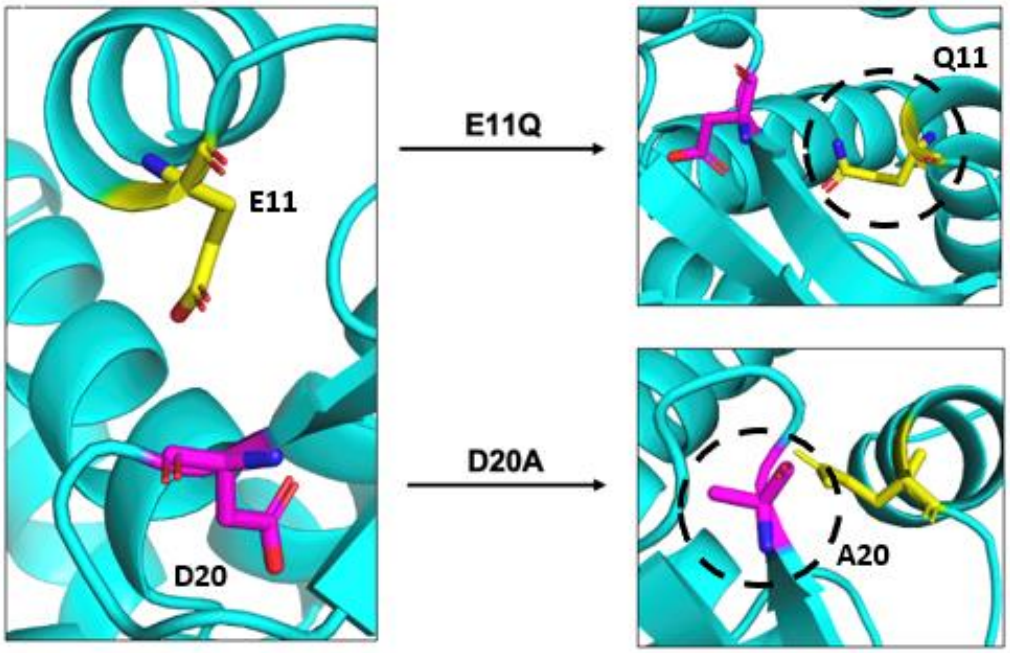

Figure 5. Representation of catalytic residues, E11 and D20, in bacteriophage T4 lysozyme (T4L). Site-directed mutagenesis was performed via QuikChange protocol and sequence verified using Genewiz Sanger sequencing. Images produced via PyMOL software.

2.3.2 Challenges in Purification of T4L mutations, E11Q and D20A

As is customary with purification strategies, challenges presented in the successful purification of either the wild-type or mutagenic constructs. Following the initial IMAC purification, when left at room temperature, the protein precipitated whereas when left in cold temperatures, TEV protease did not successfully cleave at its recognition site. Initially, it was thought the 10 poly-histidine tag may restrict protease binding via a confirmational fold or by spurious interaction with the protein that prevents TEV access. Attempts to rectify this involved the use of varied concentrations of NAG to

displace this fold while allowing for TEV protease to bind. Coomassie and western blotting analyses also indicated unsuccessful cleavage. (Figure 6)

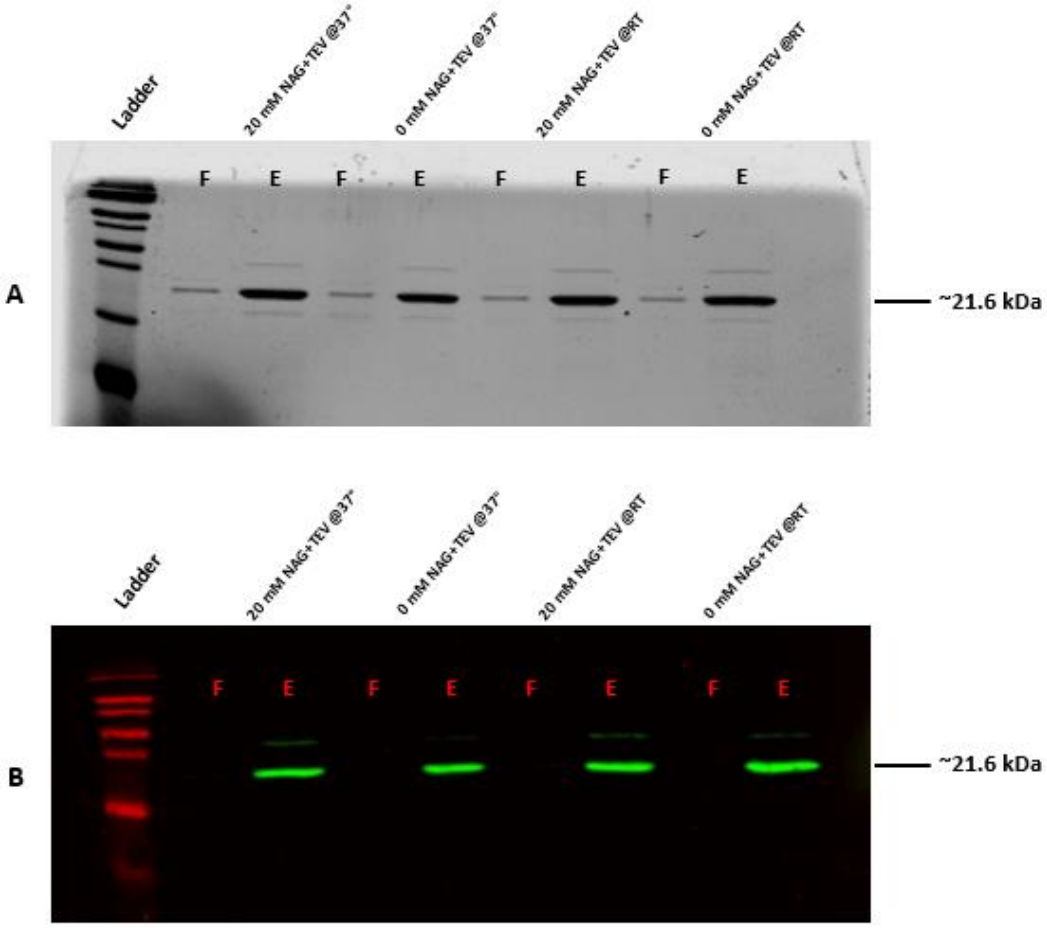

Figure 6. Coomassie blue staining (a) and western blot (b) of his-tagged T4L and NAG studies. Gel was run after IMAC II purification to assess successful cleavage of histidine tag. Lanes are as follows from left to right: protein ladder, 20 mM NAG+TEV @37 °C, 0 mM NAG+TEV @37 °C, 20 mM NAG+TEV @RT, and 0 mM NAG+TEV @RT. Flow-through **(F)** and elute **(E)** fractions are presented and indicate unsuccessful TEV cleavage via NAG competition. Expected size of his-tagged T4L is ~21.6 kDa.

Given these standard strategies were unable to effectively cleave the upstream his-tag, mutagenesis was revisited in the form of an *indel mediated frameshift* which involves the insertion/deletion of bases in the genome of the target organism. Two sets of

primer pairs were constructed; the first of which promoted a frameshift by the removal of a single '*c*' nucleotide providing the following sequence change [MSHHHHHHHHHH → MSTITIXXXXXX]. A subsequent, realignment of the T4L sequence incorporated the insertion of this same '*c*' nucleotide following the TITI stretch, producing the final sequence [MSTITIHHHHHH]. Through this strategy the 10 poly-histidine tag was successfully reduced to 6 without the need for additional subcloning. By reducing this his-tag, protein stability was obtainable at 4°C while affording TEV protease to bind in its respective cleavage site.

2.3.3 Verification of Successful Purification of all T4L Constructs

Though seemingly difficult, this new construct successfully purified using a buffer system commonly used in the Leeper laboratory for purifying inhibitor of vertebrate lysozyme (paIVY) proteins. This can be seen from the degree of separation between absorbance wavelengths λ_{255} and λ_{280} on each chromatogram. (Appendix A.2) Furthermore, Coomassie staining indicates a successful removal of remnant debris in the purification strategy yielding a relatively pure sample of T4L at the expected size of 18 kDa as a result. (Figure 7a) Western blotting provides evidence in successful cleavage of the poly-histidine tag as the latter lanes exhibits no antibody fluorophore, demarked in green. In the 'IMAC elute' lane, two fluorescent bands appear; following successful cleavage of the poly-histidine tag, TEV protease can be visualized alongside such due to it containing a histidine tag as well. (Figure 7b)

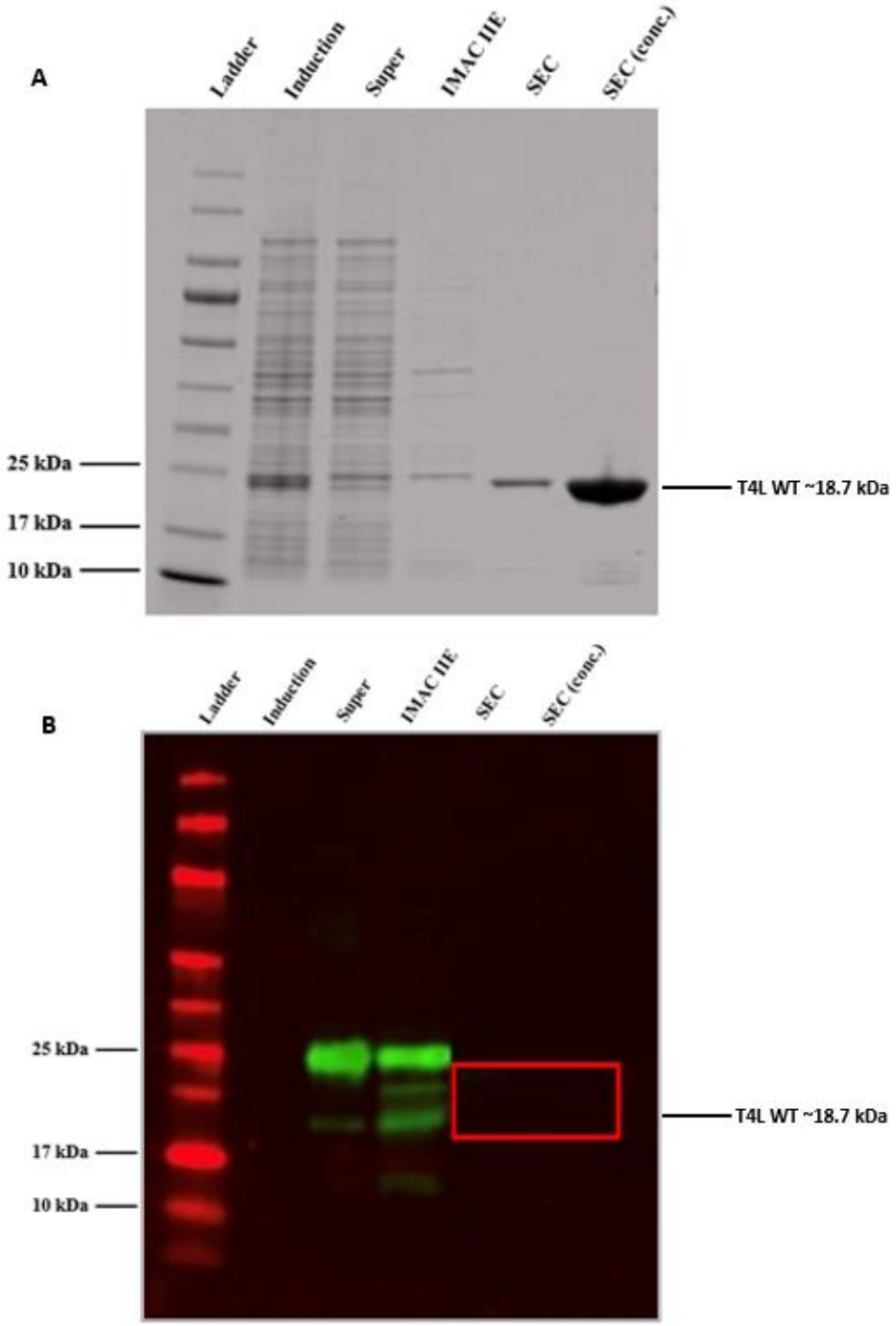

Figure 7. Coomassie blue staining (a) and western blot (b) of T4L wild type. Gel imaging followed SEC purification to assess both protein purity and visualization of histidine-tagged antibodies. Lanes are as follows, from left to right: protein ladder, induction, supernatant, IMAC II elution, SEC sample, and concentrated SEC sample. Expected size of T4L is ~18.7 kDa. Primary antibodies used in **(b)** were mouse anti-polyhistidine; secondaries were anti- mouse IgG (green) and anti- goat IgG (red).

CHAPTER III – PROBING NATIVE FUNCTION AND CONJUGATED POLYMER FORMATION VIA MURAMIDASE AND KINETIC ASSAYS

3.1 Introduction

With the incorporation of mutagenesis, the intrinsic properties unique to the target protein may become compromised, potentially inhibiting innate functionality. As mentioned in Chapter I, lysozymes inherently contribute to the hydrolysis of the β-1,4 glycosidic linkages between NAG and NAM subunits located within peptidoglycan as well as play a pivotal role regarding host immune systems.[12] Though each construct was successfully purified, preservation of lytic capacity has yet to be identified. Traditional means of assessment rely upon an activity assay referred to as a muramidase assay.

Muramidase assays measure normal lysozyme activity on fluorescently labelled *Micrococcus lysodeikticus* cell walls, where initial fluorescence is quenched until released by cell wall degradation.[31] As these cells interact with lysozyme, the integrity of the cell wall deteriorates, thus releasing a fluorophore proportional to the lytic activity present within the reaction. The emitted fluorescence can then be mapped for further quantification. As a result, mutagenized constructs can be assessed against the respective wild-type strain in determining whether variable changes to certain residues may influence the native function of lysozyme.

Beyond lysozyme's adapted activity on cell walls, we seek also to understand the catalytic mechanism driven by these lysozymes to produce a conjugated polymer. In

crystallographic studies, considerable quantities of poly-2-EP can be seen accumulating near and around the expected active sites of HEWL – this will be later explored in Chapter V. Furthermore, early kinetic data visualize the formation of polymer for HEWL occurring around 541 nm thus providing a foundation of the spectral range to investigate during the T4L kinetic trials. (Appendix A.1) From a monomeric standpoint, 2-EP is quite small (F.W. 103.12 g/mol); however, whether this monomer polymerizes via a processive/ semi-processive mechanism or by the joining of partially polymerized blocks remains elusive due to polydispersity in the polymer product lengths. Polydispersity is a trying feat in attempting biophysical characterization as it is nearly impossible to isolate the individual, length polymers within the system. Nascent kinetic trials were conducted to screen for optimal concentrations and conditions viable for polymer proliferation; from these, kinetic parameters were multiplexed and monitored to assess the genesis of conjugated polymer elicited by each mutagenic strain.

3.2 Experimental Design

3.2.1 Muramidase Activity Assay

In preparation for the assay, a working stock of DQ lysozyme substrate, fluorescein conjugate cells (Sigma Aldrich, St. Louis, MO) were prepared to a final concentration of 50 µg/mL. Assays were performed at 25ºC in 96-well, clear-bottom microplates. For each experiment, ten wells were initially loaded with 50 µL of DQ working stock. Purified T4L proteins, obtained from Chapter II, were incorporated by loading 50 µL of protein to the first well and performing a serial dilution, with each subsequent well receiving 50 µL of the previous wells' mixture. Assays were then covered using aluminum foil and left to incubate for 30 minutes. Fluorescence reads

(excitation 485 nm/emission 530 nm) were taken at the 30-minute interval and background subtracted via Gen5.2 software to assess lysozyme activity.

Data obtained from the assays were exported into GraphPad Prism software and tabulated. Representative data detailing the variance in lysozyme activity of each mutated T4L strain are shown in text and were performed following each purification, totaling three assays for each mutant to report statistical significance.

3.2.2 Polymerization Assay Design and 2-EP Kinetics

The overall objective of this project is to test if T4L can polymerize 2-EP. While the above activity assays can validate if enzymatic activity is maintained, separate and quite different assays are required to determine the rate of 2-EP polymerization. Optimization trials began by diluting purified wild-type T4L, obtained in Chapter II, to three, working concentrations of 125 μM, 250 μM, and 500 μM. Similarly, varied concentrations of 2-EP were selected to screen an array of experimental parameters – concentrations of 2-EP were 60 mM, 90 mM, 100 mM, 120 mM, 150 mM, and 180 mM, thus providing 18 screening conditions. As experimental success weighed heavily on accurate lysozyme to monomeric 2-EP molarity ratios, concentrations of both T4L and 2-EP were analyzed using GraphPad Prism software and tabulated prior to each experiment to visualize kinetic profiles of these conditions. (Appendix A.3)

2-EP kinetic experiments were performed at 25ºC in nuclease-free water in 96-well, clear microplates and sealed with Roche 480 sealing films (Millipore Sigma, Burlington, MA). For each experiment, calculated amounts of wild-type T4L, 2-EP, and water were vortexed to ensure homogeneity and prepared to a final volume of 225 μL, of

which 200 μL were loaded into their respective wells. In addition, each experiment included two controls: an enzymatic control – one well using HEWL instead of T4L – and a polymeric control – one well with no 2-EP. Polymer accumulation was monitored every hour for a duration of 8 hours via endpoint read using a microplate reader. Data obtained were analyzed, as detailed in 3.2.1, with analyses represented in text.

From these data, optimal concentrations of T4L and 2-EP were identified; as such, all purified strains were prepared, loaded into 96-well, clear microplates and sealed as before. Polymer accumulation was monitored via a spectral scan ranging from 300 nm to 550 nm spanning three days until saturation. These data were compiled for each mutation and analyzed using GraphPad Prism software. Further explanation and design parameters are extensively detailed in Appendix C.

3.3 Results and Discussion

3.3.1 Mutagenesis Perturbs Natural Muramidase Function

Single nucleotide mutations have been shown to interfere with protein structural integrity as well as perturb native functionality,[32] leading to improper folding and mitigated activity, with some instances rendering the protein's intrinsic aptitude inactive. Activity assays performed in this study illustrate a compelling case in support of this. Although lytic potential is present, a significant decrease can be seen from the E11Q variant to that of the D20A mutant, more so when compared to the initial, wild type. (Figure 8) From these data, mutated variants of T4L elicit lower lytic activity, that is, in tampering with these catalytic sites, lysozyme's inherent ability to lyse the linkages within peptidoglycan is compromised. As E11Q exhibits a greater loss of activity than

that of its counterparts, this suggests the E11 active site may considerably contribute to lytic capacity over the D20 locale.

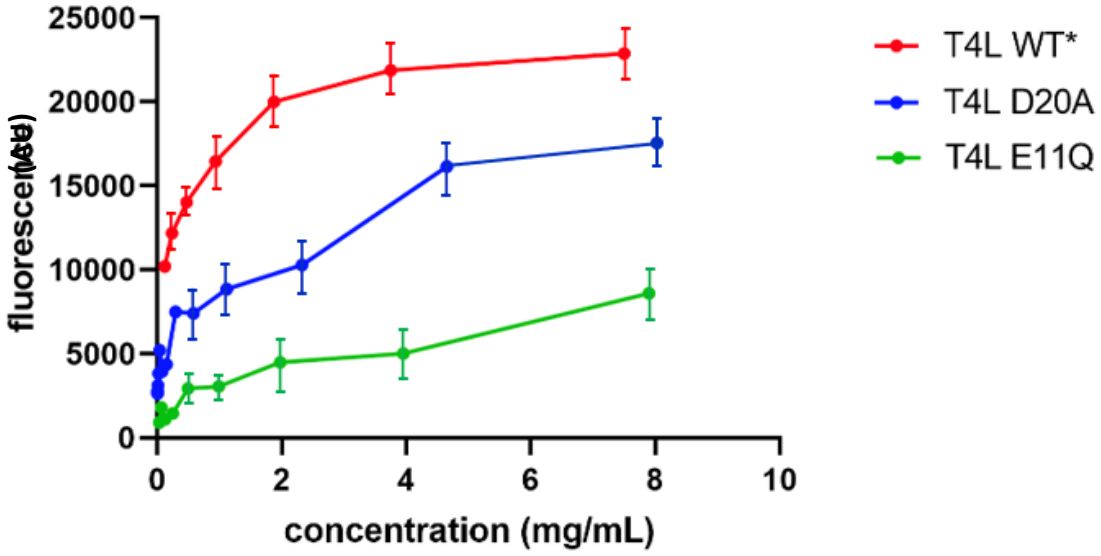

Figure 8. Detection of lysozyme activity using the EnzChek Lysozyme Assay Kit. Increasing amounts of lysozyme were incubated with the DQ lysozyme substrate for 30 minutes at room temperature. The fluorescence was measured using a microplate reader using excitation/ emission of 485/530 nm. A background fluorescence was subtracted from each value.

3.3.2 Optimization of polymerization function: 2-EP + T4L Kinetic Parameters

Though polymer accumulation was observed using the initial concentrations of each purified variant, with concentrations ranging from high micromolar to low millimolar, the rate at which this occurred was too fast to be determined. To rectify this, wild-type T4L was diluted to the three concentrations denoted; HEWL served as the positive control due to its known ability to catalyze this reaction whereas wells null of lysozyme acted as the negative control for each condition, supporting the enzymes necessity in driving this mechanism forward.

Accumulation of conjugated polymer occurred over the next several hours, with reactions being monitored every hour for the first eight hours, and then once at 24 hours when most reactions had reached saturation. In looking at the plate, higher concentrations of both lysozyme and 2-EP produced higher yields of the polymer; however, some of these exhibited early precipitation at T_0, the most notable seen in 500 μM lysozyme paired with 2-EP values higher than 100 mM. (Figure 9) Values of each 2-EP reaction were plotted against their respective lysozyme concentrations and analyzed to assess when ratio of each were necessary for future experiments.

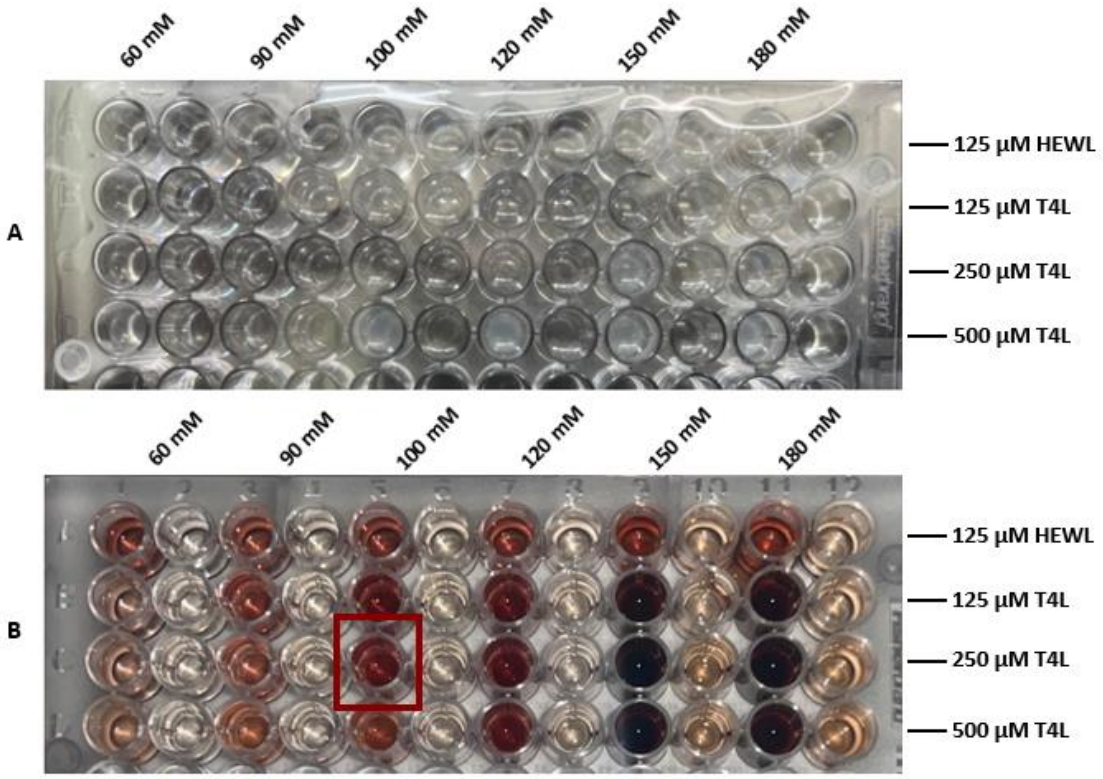

Figure 9. Kinetic assays using wild type T4L to determine optimal ratios of protein to 2-EP for assessing polymer accumulation. Wells are as follows, from left to right: 60 to 180 mM 2-EP, with a control well consisting of water and 2-EP of the same concentration for each. Variable concentrations of T4L were tested (125, 250, and 500 µM) with low concentration HEWL serving as a control. Initial observations at T_0 show early precipitation at higher concentrations of either variable. **(a)** Red hue, indicative of polymer formation, can be visualized 24 hours later. **(b)** The condition isolated in the red box was found to be the best condition for future experiments.

In knowing HEWL performs similar chemistry, mimicking its kinetics may afford insight into what conditions T4L must meet to elicit similar results; Figure 10 illustrates each of the kinetic profiles described. From these data, at lower concentration of enzyme (T4L), a saturation state occurs when combined with higher concentrations of the substrate (2-EP). Due to the presence of high substrate, this limits the enzymes' ability to effectively catalyze this reaction and further expound upon its kinetic profile. However,

in increasing the concentration of T4L, saturation occurs, with both 250 μM and 500 μM providing viable conditions. In comparing the rates of polymer formation, at higher concentration of enzyme, rate of polymer accumulation slows suggesting a reciprocal notion to that of lower enzyme reactions. Thus, optimal concentrations of both T4L and 2-EP were determined for kinetics, 250 μM and 100 mM, respectively.

In application, each T4L variant was diluted to a concentration of 250 μM, doped with 100 mM 2-EP, and read intermittently over the next 48 hours. Initial readings yielded weak absorbance indicating low polymer accumulation; however, subsequent readings showed gradual propagation around the 400 nm region thereafter. (Figure 11) Of these mutants, wild-type and E11Q achieved a greater propensity in forming polymer whereas D20A exhibited a rate nearly, half that of the former two. With the reduction of 2-EP polymerization, these data suggest the D20 residue may be more important to the lysozyme's catalytic efficacy for polymerization, in contrast to its lytic muramidase activity.

Though not conducted here, other potential mutants, such as D20N – similar construct to that of E11Q – or a double mutant, may be integrated to affirm these outcomes to probe how other iterations could influence either the lytic or 2-EP polymerization potential of T4L.

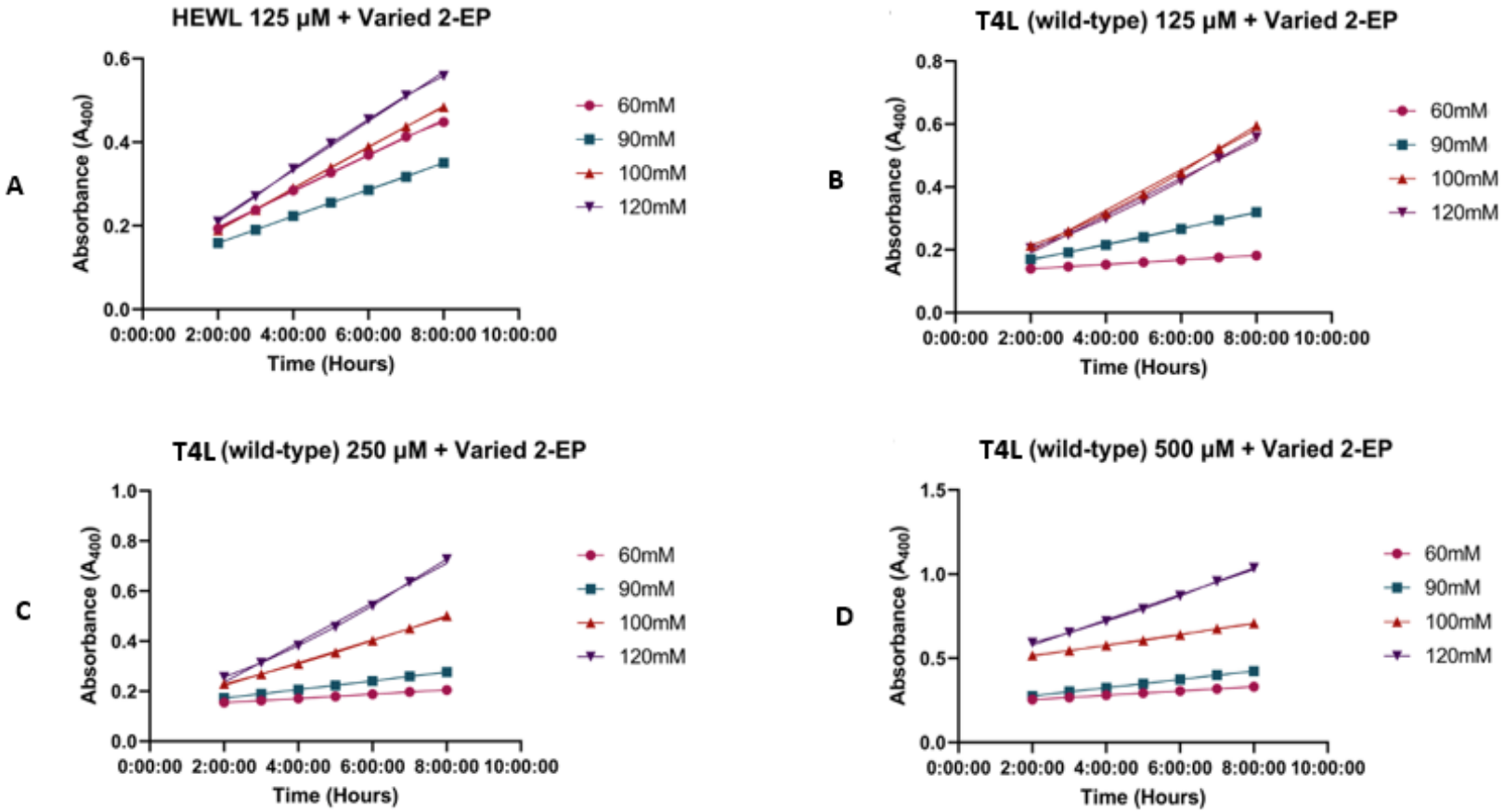

Figure 10. Kinetic profiles of varied T4L concentrations investigated in Figure 9. HEWL acted as a control for comparative analyses. **(a)** Polymer accumulation rates were taken every hour for a duration of 8 hours and plotted as shown. Upper concentrations of 2-EP were omitted due to inaccurate readings or rates being too fast to accurately obtain. Panel **B** shows a level of saturation being achieved in the presence of low T4L concentrations whereas panel **D** show a relatively fast rate of polymer accumulation. Panel **C** serves as a likely candidate for lysozyme concentration with 100 mM giving an optimal rate to monitor polymer accumulation.

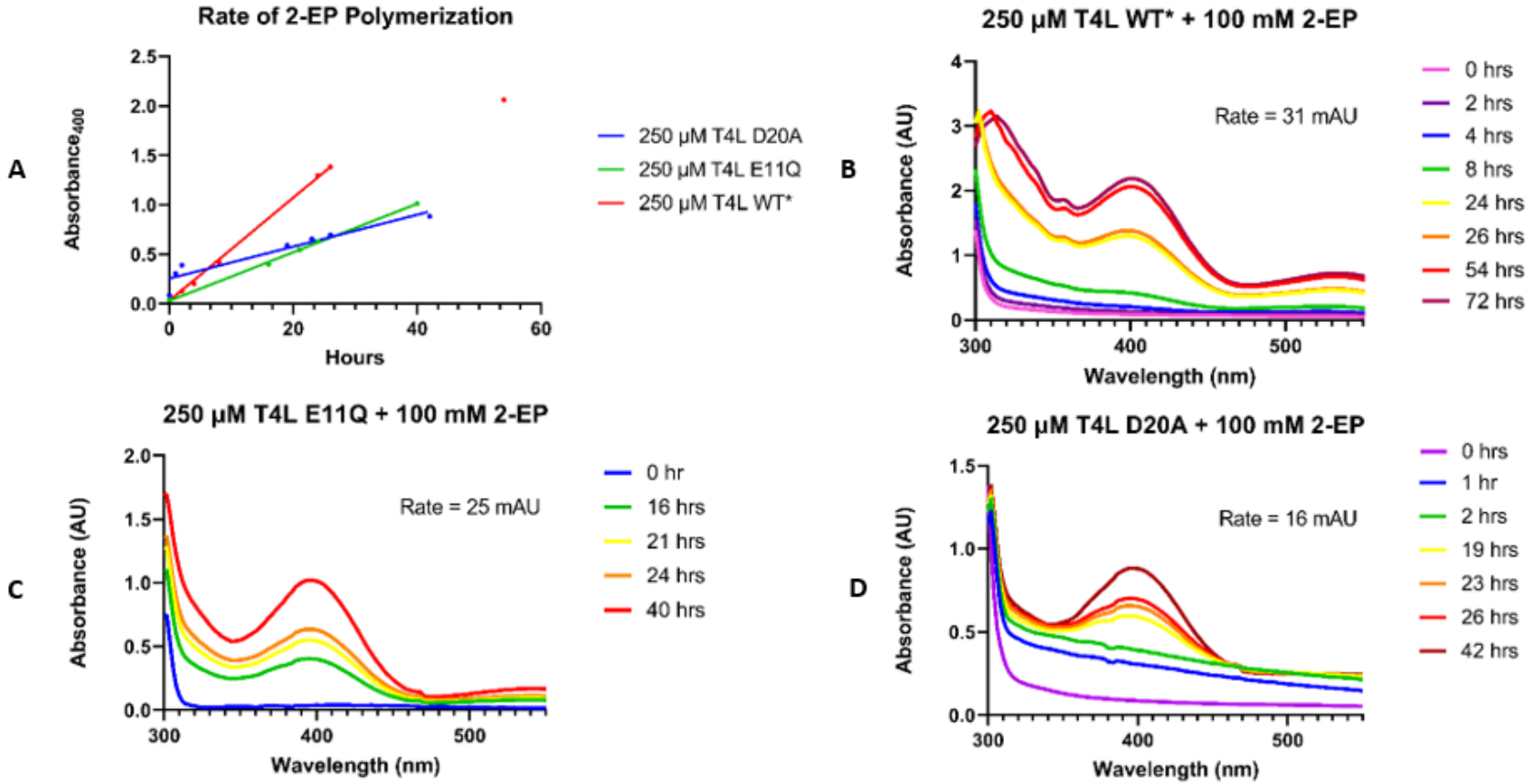

Figure 11. Mutagenized T4L protein's ability to polymerize 2-EP to form a conjugated polymer. Polymer accumulation occurs around 400 nm; this is different than that of HEWL's accumulation occurring around 541 nm. This supports that either lysozyme's product is different per the varied intervals of conjugation, with HEWL being more conjugated than that of T4L. The value corresponding to this at each interval were plotted for each and graphed to assess rate of polymerization, shown in **(a)**. Each experiment was background subtracted and simple linear regression was applied to receive each mutation's product accumulation rate. **(b-d)** Visible variation can be seen in mutating active site residues in comparison to the wild type.

CHAPTER IV — BIOPHYSICAL CHARACTERIZATION OF T4 LYSOZYME

4.1 Introduction

Various structure determination techniques and instrumentation have led to the deposition of thousands of structures in recent decades; however, the function of many of these proteins are either unknown or inferred from their respective amino acid sequences.[25] In the case of enzymes, even less is known about their substrate specificities and often go uncharacterized. To elucidate the mechanism of 2-EP polymerization by these lysozymes, several biophysical techniques were undertaken to assess polymer-protein interactions, binding affinity, and thermodynamics.

Nuclear magnetic resonance (NMR) is a powerful method well-known for its ability to solve macromolecular structures[26] as well as allow for the determination of enzyme-substrate interactions. One of the most common experiments using NMR involves a 2-dimensional pulse sequence known as a heteronuclear single quantum coherence (HSQC). The HSQC allows for the assignment of the amino acid residues of a given protein (with the exception of prolines), with the chemical shift of each peak dependent upon the chemical environment within said protein. To accomplish this, proteins are isotopically labelled to increase the resolution of signal to noise and promote a higher concentration of spin active nuclei. The spectrum supplements as a fingerprint of the folded protein and can be used to monitor protein interactions that occur via the titration of unlabeled ligand; in turn, this can afford residue specific information about the variable chemical changes.

As chemical shift change is very sensitive to structural changes found within these experiments, binding interactions between ligand and protein will often produce chemical shift perturbations (CSPs)[27] that can be used to infer which residues of the protein are contributing to various chemical mechanisms. Although CSPs are revealing, the understanding of binding affinity is limited to that of very weak binders (i.e. high micromolar to low millimolar K_D values) due to the limitations on protein concentration. Incorporating complimentary techniques can provide additional information, such as overall affinity and thermodynamic properties, that NMR cannot.

Biolayer interferometry (BLI) is an optical technique that measures the interference pattern obtained via the combination of light reflected from a biolayer and an internal reference surface.[28] This technique uses a biosensor affixed with streptavidin ligand that is placed into a well with the biotinylated analyte of interest. Association and dissociation of analyte to and from the ligand changes the light interference pattern, generating corresponding curves that provide information regarding the on/off rates and affinity. From this approach, BLI can provide information of the affinity and stability of interactions as well as determine the rate constants of the binding reactions.

Complimentary to BLI, isothermal titration calorimetry (ITC) is a technique that establishes various thermodynamic parameters in relation to binding interactions, such as affinity, enthalpy, and stoichiometry. Titrating one reactant into another produces a signal coordinating with the heat absorbed or released upon the binding.[29] A series of injections are performed and, as the limiting reactant saturates, the signal intensity will eventually reach saturation yielding a spectrum consistent with a sigmoidal curve thus affording insight into the unique properties of the proteins' thermodynamics can be ascertained.

In this chapter, NMR indicated proper folding of the purified mutagenized T4L proteins from Chapter II and, coupled with peak assignment, determined which amino acid residues are exhibiting CSPs from the incorporation of 2-EP monomer. Further biophysical characterization assessed binding affinity, thermodynamics, and stoichiometry using complimentary techniques to the former, BLI and ITC.

4.2 Experimental Design

4.2.1 ^{15}N HSQC Samples

Samples were prepared at a protein concentration of 250 µM and diluted using 99.9% deuterium oxide (D_2O) (Cambridge Isotope Laboratories, Inc., Tewksbury, MA) to produce an 8% D_2O mixture, in a final volume of 500 µL. Solutions were transferred to NMR sample tubes and labelled accordingly. Initially, samples were processed via 2D TROSY HSQC using a Bruker Ascend™ 600 MHz NMR; pulse program parameters are detailed in Appendix D. Following the baseline HSQC, 100 mM of 2-EP monomer was added to the samples and subsequent scans taken using the same parameters. Spectral scans were taken every 24-hour increment for a duration of 7 days; these were processed using Bruker TopSpin and analyzed using biomolecular NMR software, SPARKY. Peaks were assigned and spectra overlayed; from this, residues exhibiting chemical shift perturbation were identified and mapped via PyMOL to visualize their locations within T4L.

4.2.2 Biolayer Interferometry Experiments

Binding kinetics were determined between poly-2-EP and biotinylated T4L by biolayer interferometry (BLI). Purified T4L served as the ligand this was accomplished by pipetting 2.5 µL of 10 mM EZ-Link NHS-LC-LC-Biotin stock solution (2 mg EZ-

Biotin; 350 µL DMSO) to 100 µL of protein. The mixture was vortexed, left to biotinylate at room temperature for 30 minutes, and then desalted to remove any residual biotin using a Zebra Spin Desalting Column, 7K MWCO, 0.5 mL (ThermoFisher Scientific, Waltham, MA) with phosphate buffered saline (PBS).

BLI experiments were performed using an Octet 96e biolayer interferometer (FortéBio, Fremont, CA) at 25ºC in 1x PBS buffer (137 mM NaCl, 2.7 mM KCl, 10 mM Na_2HPO_4, 1.8 mM KH_2PO_4, pH: 8.0) in 96-well, black-bottom microplates (Millipore Sigma, Burlington, MA). For each experiment, 2 µM biotinylated T4L variants were immobilized for a 5-minute incubation onto Streptavidin biosensors (FortéBio, Fremont, CA) which were hydrated in 1x PBS buffer 60 seconds prior. Loaded biosensors were rinsed in fresh 1x PBS for 5 minutes to establish immobilized baselines, then immersed in 1x PBS buffer containing 2 µM poly-2-EP for an additional 5 minutes, and finally washed in fresh, 1x PBS buffer for 10 minutes. Biosensor data for each experiment were obtained every 0.2 seconds and recorded in wavelength shift (nm). Each experiment included two parallel controls: a non-specific binding control in which the sensor without T4L was exposed to analyte and a baseline control in which a T4L-loaded sensor was only exposed to buffer throughout the experiment. Data obtained from the controls were subtracted from the experimental data prior to analysis and graphed using GraphPad Prism software.

4.2.3 Competitive Isothermal Titration Calorimetry Design

In addition to binding kinetics, thermodynamic parameters and stoichiometric values were investigated using competitive isothermal titration calorimetry (ITC); all experiments were conducted using a NanoITC (TA Instruments) in 18 MΩ H_2O. Optimal

starting concentrations of ligand to protein were estimated with a c-value of 10 serving as the ratio between protein concentration and assumed dissociation constant for each mutagenized protein using Equation 1; *n* is the numerical value of ligand that will bind to protein and K is the binding constant.

$$c = \frac{n\,[titrant]}{K_d} \qquad \textbf{Equation 1.}$$

Both $(NAG)_3$, a ligand with high affinity for lysozymes, and T4L samples were prepared to concentrations of 1.115 mM and 0.150 mM, respectively, and doped with 10 mM poly-2-EP; samples were subsequently filtered and degassed for 10 minutes then loaded into the reference cell at a volume of 300 µL. Thermodynamic calculations were produced via a titratable volume of 185 µL. Prior to experimentation, the instrument was allowed to reach a baseline while the syringes stirred at 200 rpm to reach equilibrium. The protein was then loaded into the sample cell at the same overfill volume. The prepared $(NAG)_3$ was loaded into the syringe at an overfill volume of 52 µL, though the volume used for thermodynamic calculations is 50 µL. After a flat baseline was reached the system began 2.02 ul incremental titrations over 22 injections. Thermodynamic data were analyzed using the TA NanoAnalyze software. Within the software, an independent analysis was performed on each experiment – one with competitive poly-2-EP ligand and the other without – to produce K_D values and assess the thermodynamic and stoichiometric profile. In addition, these spectra were overlayed to assess any changes that may have occurred.

4.3 Results and Discussion

4.3.1 Chemical Shift Perturbations Allude to a Substrate Binding Groove

The initial spectrum of native T4L, shown in green in Figure 12, indicated both proper folding of the protein as well as conservation of chemical shifts relative to previously published HSQC spectra.[30] Incorporation of 2-EP monomer showed multiple chemical shift perturbations over the duration of the experiment; the assigned residues experiencing these perturbations were then colored over the surface plot of the published T4L structure (PDB: 2LZM) to provide insight into which residues might be influencing the formation of the conjugated polymer – this is denoted in black.

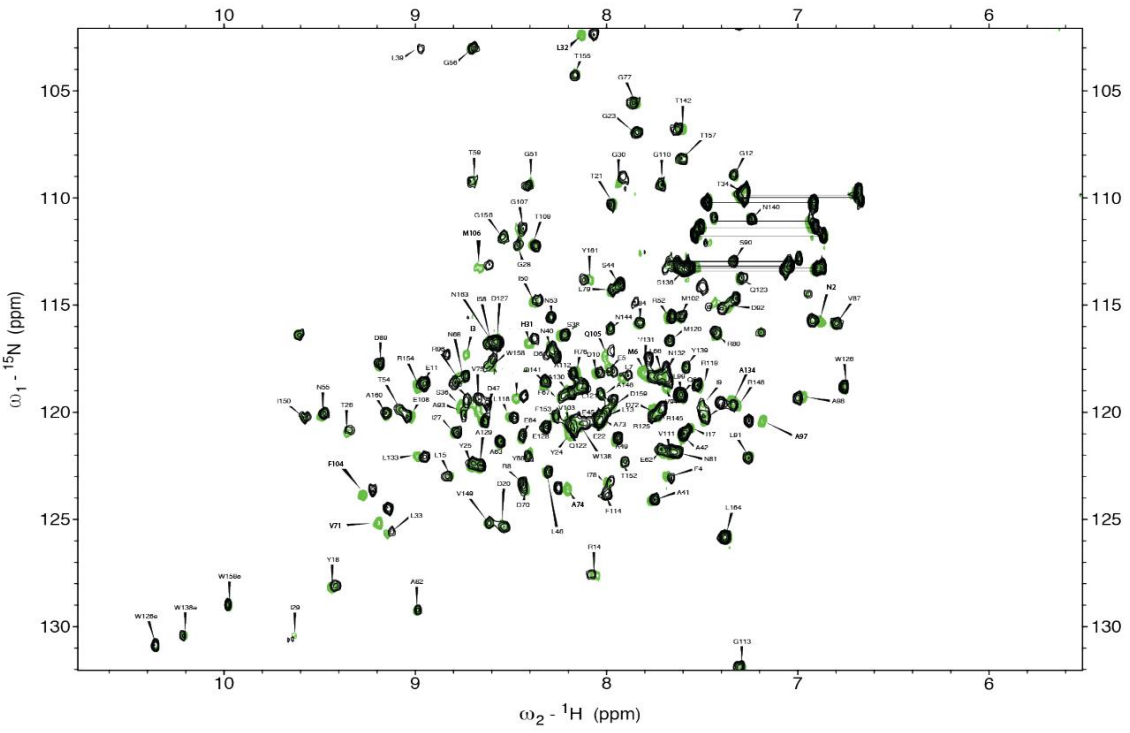

Figure 12. ^{15}N HSQC of wild type T4L overlayed with spectrum including 100 mM 2-EP. Spectrum suggests proper folding of the protein based on signal to noise and high conservation of peaks when compared to that of literature HSCQs of this protein. **Green** peaks are indicative of native T4L prior to the addition of 2-EP; **black** peaks showcase chemical shift perturbations as the polymerization of 2-EP occurs within the sample tube. Peaks assignments and overlay of spectra were conducted using SPARKY.

When mapping these residues to the structure, most of these perturbations occur within the interface between the *N*-terminal and *C*-terminal lobes of T4L, suggesting this groove is host to the binding of 2-EP substrate. (Figure 13) Within these residues, both E11 and D20 are located on either side of the binding groove and further support the findings in Chapter III, that is, in replacing these with other residues, the protein's catalytic efficacy is decreased. This suggests that while the chemistry, and hence mechanism, for 2-EP polymerization is quite different from glycoside hydrolysis the active site is conserved.

Although information can be drawn from these findings, other properties exhibited by T4L, such as the binding affinity and thermodynamic aspects of the protein, remain inconclusive and without such leave the polymerization mechanism elusive. As NMR is a technique utilized to assess weak binding affinity, complimentary techniques were undertaken to explicate other potential affinity binders as well as understand its thermodynamics.

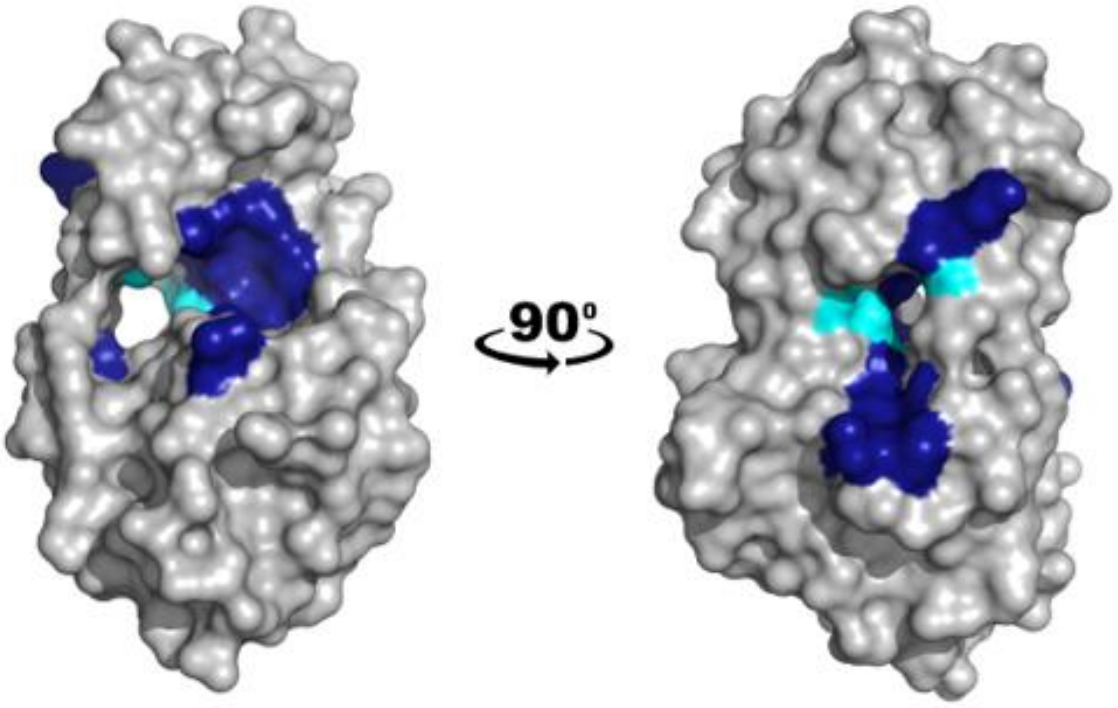

Figure 13. Residues exhibiting chemical shift perturbation mapped to structure of T4L (PDB: 2LZM). High localization of these can be seen between the interface of the two lobes **(navy)**. Catalytic residues, E11 and D20, exhibited CSPs and are denoted on either side of this substrate binding groove in **(cyan)**. Images provided via PyMOL software.

4.3.2 BLI Affords No insight into Affinity for Conjugated Polymer Formation

BLI assays were performed in attempt to characterize the binding affinity of purified poly-2-EP – obtained via liquid-liquid extraction from previous HEWL/2-EP studies – to T4L and investigate how binding is potentially impacted by mutagenesis. In these experiments, real-time binding kinetics for each mutagenized T4L were measured by recording wavelength shifts in biosensor-reflected, interference patterns brought about from the interactions of 2-EP with biosensor-immobilized protein. Raw wavelength shift data collected during these experiments at concentrations of 2 μM biotinylated T4L to 2

μM poly-2-EP were used to calculate the binding kinetics between poly-2-EP and the T4L variants tested. (Figure 14)

From these data, results were unyielding in either binding or kinetic assessment. Though some semblance of binding can be seen in panels A and B of Figure 14, the "pseudo-binding" represented by the poly-2-EP control in all panels is problematic as it elicits similar, if not higher, affinity than that of the experimental T4L to poly-2-EP, which is improbable – this is likely caused by non-specific binding of the poly-2-EP to the tip of the biosensor. It is difficult to speculate how non-specific binding occurred, however, these data provide no additional insight into the affinity either lysozyme or poly-2-EP have for each other. Additional controls and protocol optimization will need to be implemented to elucidate this aspect of the project.

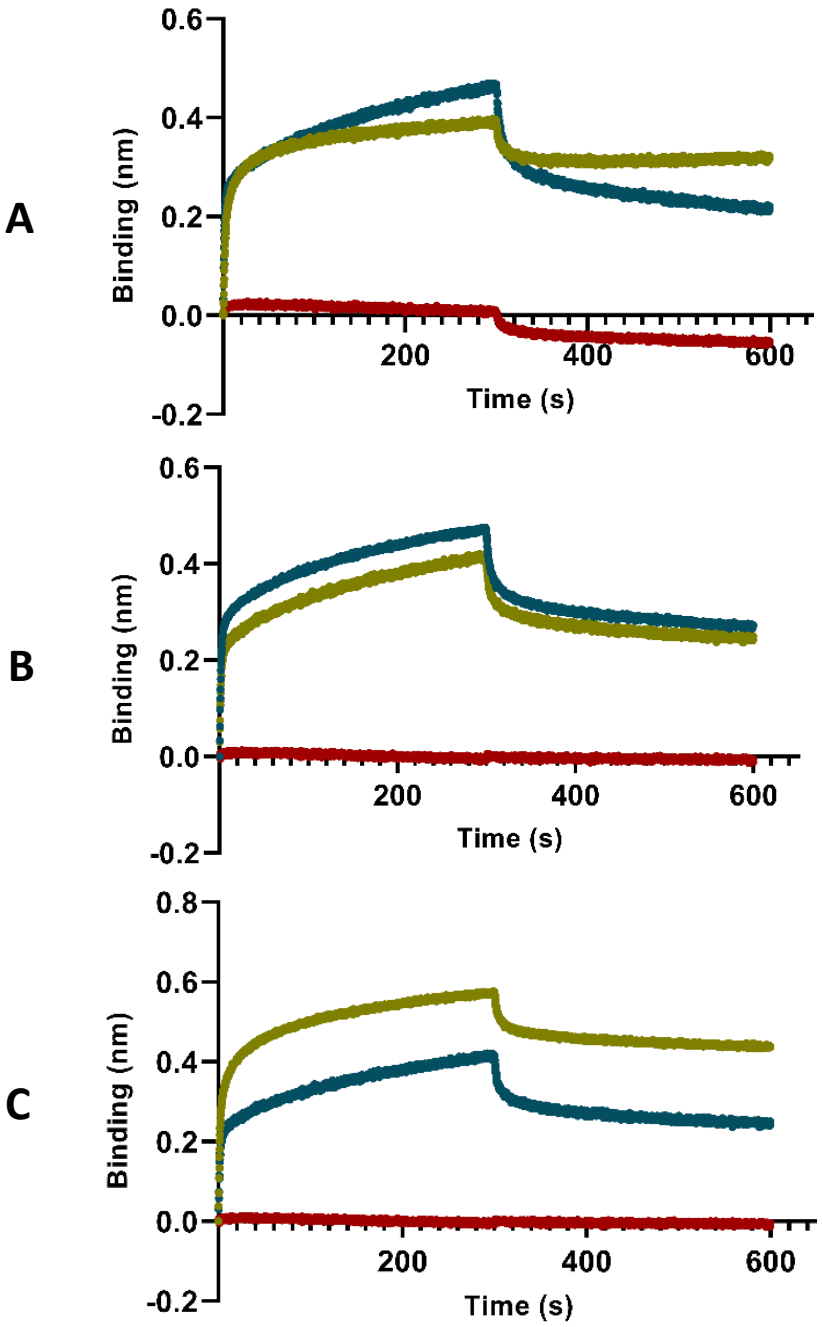

Figure 14. Representative BLI association and dissociation step raw data plots of poly-2-EP binding. Graphs depict raw association and dissociation step data measured during BLI experiments with poly-2-EP and **(A)** wild-type, **(B)** D20A, and **(C)** E11Q biotinylated proteins. Solid lines depict calculated best-fit lines for the raw data points. Blue indicates biotinylated T4L protein - wild-type, D20A, and E11Q, respectively – and yellow and red indicate controls null of analyte or ligand – poly-2-EP or T4L, respectively.

4.3.3 (In)conclusive Binding Affinity Exhibited via ITC

ITC experiments were implemented to further assess binding affinity of poly-2-EP as well as determine the thermodynamic and stoichiometric properties it presents. For each mutant, experimental values were measured via the titration of $(NAG)_3$ into T4L to out-compete the poly-2-EP bound to the protein within the sample cell and observed at 25 °C; these spectra were then overlayed to assess differences between each variant in comparison to the control, $(NAG)_3$ into T4L null of poly-2-EP. (Figure 15) From the raw data, wild-type exhibit peaks consistent with that of thermal exchange between the titrant and T4L with each normalized fit data producing standard, sigmoidal curves, final molar ratios of 2.2, and *n*-values ≥ 0.970.

In relation to binding kinetics and thermodynamics, both spectra yielded nearly identical data, whether poly-2-EP was present or not. Independent models provided a K_D value of 14.75 μM $\pm$ 0.26, ΔH values averaging -51.5 kJ/mol, and ΔS values $\geq$ 79.95 J/mol·K. These data suggest each T4L experiment exhibited exothermic properties, as supported by the ΔH and peak representation, as well as imply weak binding between the poly-2-EP and T4L. It is unclear whether these experiments conclude a 'true' weak binding correlation as the polydispersive nature of 2-EP may be interfering with binding potential.

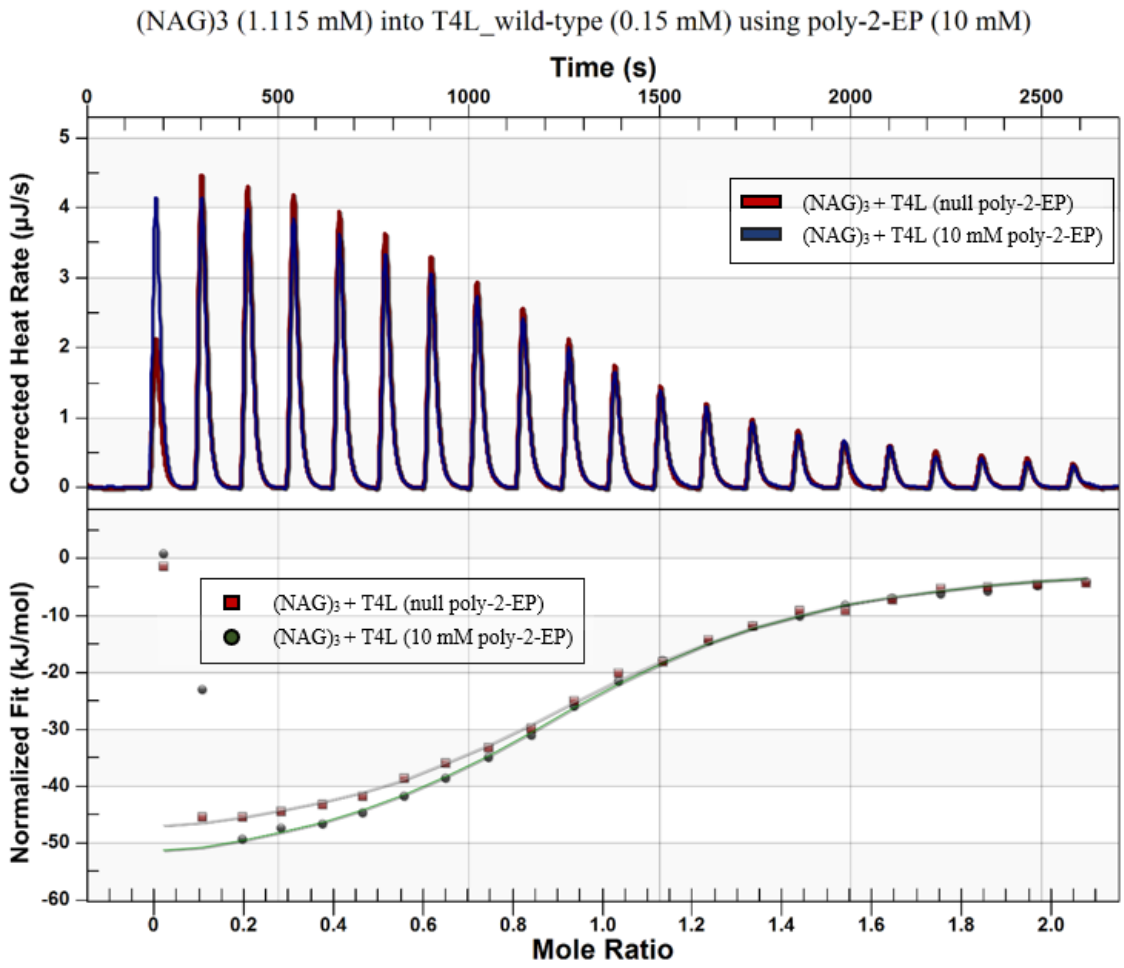

Figure 15. Titration of 1.115 mM $(NAG)_3$ with 10 mM poly-2-EP into 0.15 mM T4L with 10 mM poly-2-EP. The corrected heat rate was observed as it related to time of each 2 µL titration of $(NAG)_3$ into 300 µL of T4L. Buffer conditions were in 18 MΩ water. Consitencies in peak height and the sigmoidal curve representative of mole ratio suggest very weak or no binding.

CHAPTER V – CRYSTALLOGRAPHIC STUDIES OF T4L COMPLEXED WITH 2-EP SUBSTRATE

5.1 Introduction

Traditional routes for structure determination of proteins and biological macromolecules rely on a technique known as x-ray crystallography (XRC). In principle, XRC is a steadfast approach in the determination of conventional, small molecules;[34] however, traditional strategies of crystal formation require modifications with respect to proteins. Conventional crystallization is dependent upon the gradual shift towards a state of reduced solubility by incorporating precipitants, such as salts, organic solvents, and variable length polymers, to influence crystal growth, nucleation, or both dependent upon the system used. Moreover, other factors effecting crystal growth on a physical, chemical, and biochemical level must be accounted for, such as temperature, pH, and post-translational modifications, respectively.[36] The collusion of these elements affords a level of labile, supersaturation that is optimal in nurturing crystals.

Obtainment of a three-dimensional structure from a crystal can afford valuable insight into initial protein dynamics and structural factors – calculated via diffraction data and electron density mapping – which can then provide the specificity of protein-ligand interactions and the elucidation of unknown enzyme mechanisms.[35]

As prefaced in earlier chapters, HEWL had been shown to be capable of mediating formation of poly-2-EP; although no crystallographic studies were conducted at the time, studies using 1,3-di(2-pyridl)propane (DPP), a mimic of the polymer

repeating unit, provided preliminary insight into the mechanism of polymerization using XRC.[33] These data show a localization of DPP bound within the active site pocket between catalytic residues, E35 and D52 – these correspond to the E11 and D20 residues found in T4L. (Figure 16)

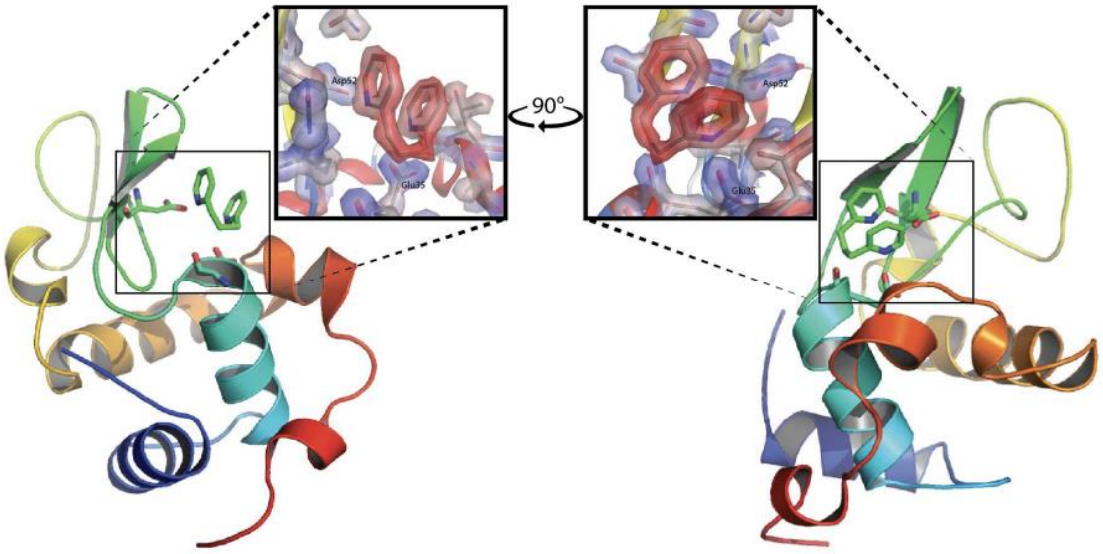

Figure 16. Prior X-ray structure of DPP bound in the active site of HEWL (PDB: 6CIW). Catalytic residues, E35 and D52, are shown in relation to the pyridine rings of DPP. Electron density mapping further illustrates the conjugated ring moiety, mimicking that of the poly-2-EP structure.[28]

Complimentary to these findings, unpublished crystallography data further supports the conservation of polymer accretion in HEWL's catalytic domain via diffraction data and electron density mapping. (Figure 17) However, the electron density attributed to the polymer only weakly diffracts or is of low occupancy, suggesting that additional studies were required to visualize the polymer's position and orientation within the lysozyme active site.

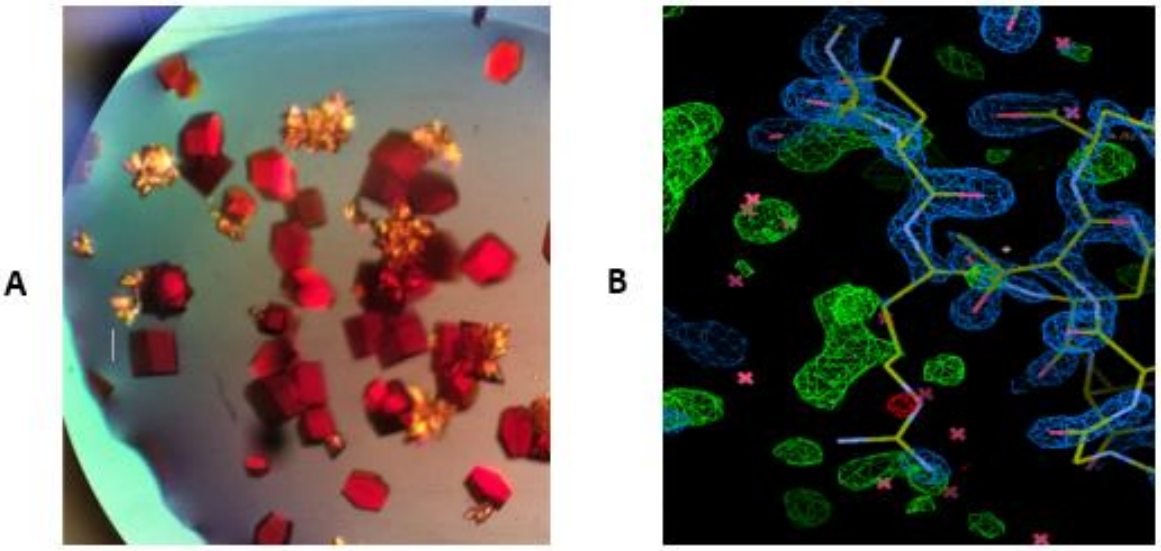

Figure 17. Crystallization of HEWL crystals complexed with 2-EP, unpublished. Brilliant red is indicative of conjugated polymer in the lattice structure. **(a)** Electron density mapping suggests low occupancy or exhibit relatively weak diffraction patterns. **(b)**

In continuation of this, as T4L has been shown to exhibit identical characteristics to that of its glycosidic hydrolase precursor, attempts to crystallize the lysozyme complexed with poly-2-EP were performed to a) isolate the complex to understand how 2-EP substrate is recognized, and b) investigate how the integration of variant catalytic residues may influence the protein's capacity to sustain this mechanism.

5.2 Experimental Design

5.2.1 Screening of Deposited X-Ray Diffraction Conditions

To determine what conditions were optimal in growing T4L crystals, a screening of published protocols in the Protein Data Bank (PDB) was initiated followed by incremental refinements to elucidate the best conditions to replicate. Parameters began by searching "bacteriophage T4 lysozyme" within the database, populating nearly 8000

crystal depositions; of these, further refinements were introduced to produce consistency amongst crystallography conditions. Parameters were refined as follows: sourced organism were limited to *Escherichia virus T4* and *Escherichia coli*, experimental methods were limited to solely x-ray diffraction, and refinement resolutions were limited to values ≤ 2.5 Å – these criteria yielded 593 structures to assess for crystallography trails.

Data files of each structure were compiled into a shell script and generated into file batches for download. Once downloaded, batch files were screened using the terminal prompt window to isolate individual crystallography conditions for each deposition; as some were unavailable via the PDB or the paper associated with such, attainable conditions were tabulated to provide a foundation for potential screening parameters. (Appendix A.4)

5.2.2 Hanging Drop Crystallography Trial Design

Prior to crystal screening, purified wild-type T4L, obtained as described in Chapter II, served as the protein stock and buffer contents with their respective additives were prepared and pH adjusted. Each experiment was conducted in a 24-well VDX crystal screening plate (Hampton Research, Aliso Viejo, CA) with each reservoir containing 500 µL of the prepared solutions being tested. Following this, 2 µL of T4L was added to 2 µL of each solution (1:1 ratio) and affixed to 22 mm x 0.96 mm square-shaped, cover slides (Hampton Research, Aliso Viejo, CA); these slides were flipped, positioned over the respective well, and, finally, secured using high vacuum grease (Dow Corning, Midland, MI). Each drop was examined immediately following the slides' placement to indicate the initial, phase assignment score – these drops were then screened

daily to assess any phase change or crystal formation for the duration of a week, both at room temperature and 4°C.

Viable crystal conditions were intended to be replicated using T4L complexed with 2-EP monomer to capture the polymerization interaction *in crystallo*; crystals would then be looped and subjected to a cryoprotectant to retain protein-crystal integrity and sent out for x-ray diffraction.

5.3 Results and Discussion

5.3.1 Challenges and Limitations in Crystallography Trials

From the hundreds of potential conditions, a select nineteen were investigated as the components within each solution were the most common amongst the successful crystal depositions – primarily those with variable poly-ethylene glycol (PEG) molecular weights, sodium to potassium phosphate ratios, and a range of relatively neutral pH values. (Appendix A.4) Additionally, hanging-drop method and colder temperature consistencies allowed for high throughput.

Initial observation of the experiment resulted in a range of outcomes. Clear drops were present in most wells alluding to no phase separation occurring from the incorporation of protein to the solution, whereas conditions involving phosphate buffers showed early phase separation visualized as small and large droplets suggesting a possible, protein-rich environment that could produce viable crystals and might be resolved using variable temperature conditions. Remaining wells – all of which encompassed the PEG conditions – either yielded an amorphous or cloudy mixture or ‘skin’ precipitate indicating denatured protein or potential oxidation between the solution and protein, respectively.

Conditions were continuously screened daily for the duration of a week, all of which yielded no crystal formation. Those that produced phase separation and no aggregation were replicated both at room temperature and 4°C at concentrations consistent with original design and lower protein concentration (1 µL:1 µL); this was proposed as reduced concentration could lower nucleation, reduce previous phasing as well as provide a more soluble environment for crystal growth. Although lower protein concentration yielded smaller phase droplets, no crystals were observed either.

Knowing phosphate buffers afforded better results, these buffers were optimized by varying the molar concentration of phosphate (1.8 M to 2.1 M) while incorporating a range of pH values from 6.5 to 7.5 in 0.2 increments. Of these, a single result from condition 2.0 M sodium phosphate/potassium phosphate, pH: 7.0, 50 mM HEDS (Millipore Sigma, Burlington, MA) via hanging-drop method at 4 °C showed very minute microcrystals. Although these provide a starting condition for growing T4L crystals, it is unknown whether these formed from salt precipitation or genuine complexing of the T4L in this buffer. Furthermore, conditions were studied for upwards of a week whereas published protocols observe crystal formation for several weeks to months.[38,39]

Future crystallography trials should take the following considerations into account. Initially, the sole condition that produced microcrystals should be replicated and identified to support these findings. Literature suggests that increasing the concentration of protein, or the amount present in the hanging drop, proportionally increases the nucleation step allowing for higher crystal potential.[37] In addition, when preparing these trays, all equipment and reagents should be stored, prepared, and imaged at 4°C to eliminate possible degradation of crystals in moving between different temperature

environments. Literature also supports the usage of HEDS over BME as the slow, reduction event encourages crystals to retain lattice integrity.[38,39]

CHAPTER VI – CONCLUSIONS AND POTENTIAL IMPACT

As demand for greener syntheses become more prominent in the forthcoming era, modifications to existing polymerization schemes as well as the development of novel approaches must be developed. From this research, enzyme-based catalysts present as a viable method in obtaining conjugated polymers by taking advantage of their unique properties in lieu of traditional metal-embedded proxies. With initial attempts in deriving the mechanistic route of these enzymes proved unyielding, this work provides data in support of discovering the elusive pathway.

Protein purifications using the initial construct of T4L and the original IEX-based protocol[19] yielded low concentrations (~12 mg) and were incapable in performing extensive characterization studies without additional purifications being conducted. Using molecular subcloning, the T4L sequence was excised and cloned into a pBAD/HIS vector that incorporated a 10 poly-histidine tag and TEV cleavage site that allowed for a 'cleave-and-clear' IMAC purification strategy to be implemented. However, this initial 10 his-tag construct proved unsuccessful in cleaving the upstream histidine tag at the TEV recognition site so further optimization was necessary. A novel approach using primers to promote an *indel mediated frameshift* allowed for the reduction of this his-tag to 6 – a more traditional sequence stretch in IMAC purification strategies. This resulted in successfully removing this stretch of sequence from target protein and significantly improved the protein yield approximately three-fold (~32 mg/mL). These made for high

throughput of analyses and afforded optimal yields for crystallization studies otherwise unobtainable. It is important to note that although extensive modifications were made to the original IEX-purified construct, all three T4L variants (his-tagged or non) were effective in producing poly-2-EP convincing us this polymerization is not unique to one particular construct over another.

Further supporting the key contribution the active site residues have in the recognition of the 2-EP monomer to then influence orthogonal conjugated catalysis, either residue was mutated to probe for altered activity both at the lytic and catalytic level. Activity assays revealed that mutating the E11 site residue to a glutamine altered the lytic capability by nearly three-fold when compared to that of its counterparts; additionally, kinetic assays suggest the D20 site is responsible for catalytic efficiency seeing as polymer accumulation was reduced nearly half that of the wild-type and E11Q variant. Due to the ionizability of both glutamic and aspartic acid as well as their ability to stabilize catatonic 2-EP or poly-2-EP, it can be inferred the combination of these residues may promote a strong recognition site for these compounds and thus influence this type of catalysis.

Biophysical characterization studies provide evidence indicative of weak binding interactions between lysozyme and 2-EP; although polymerization is highly localized within the groove between either lobe, the proximity of each may strongly influence rapid catalysis between monomers. As alluded to in Chapter IV, binding studies using BLI and ITC suggest little to no binding but whether this can be inferred as an accurate representation is uncertain due to the polydispersive nature of 2-EP as it is difficult to isolate individual, length polymers within the system and assess how a uniform polymer

environment may influence certain attributes– at least, using traditional biophysical strategies.

Crystallography afforded a single condition producing microcrystals that were unable to be identified as either salt precipitate or genuine crystallization of T4L. Variable conditions were considered and tested to provide a foundation for continual studies to isolate the recognition site of the 2-EP monomer.

Future Directions

Taken together, these data support that other enzymes support poly-2-EP polymerization. More work need be pursued to further support these findings. For example, complimentary mutations, such as D20N, E11A, and a double alanine mutant, may show how these key residues contribute to 2-EP polymerization. These data will be assayed and compiled with current variant results. In addition, other related enzymes, such as bacteria chitinases that are related to chicken and viral lysozymes in mechanism and sequence [24] should be screened for 2-EP polymerization activity.

Future biophysical characterization is necessary to further explore the true binding and thermodynamic aspects of the protein. As poly-2-EP is polydispersive, the traditional BLI and ITC experiments described here are difficult to effectively apply and analyze. However, in isolating variable lengths of polymer, using methods such as gel permeation chromatography (GPC), these may be more applicable to standard protocols and provide better insight into these unknowns.

Additional NMR experiments can be revisited in determining binding affinity using saturation transfer difference (STD) NMR. With this experiment, titrations of

ligand into the system can provide ligand resonance signals that can then produce a binding epitope useful in the K_D determination of weak binders.

Another important aspect for consideration would be continuation of crystallographic studies. The condition that produced microcrystals should be screened around to determine the optimal conditions using suggestions alluded to at the end of Chapter V. These crystals can then be harvested and sent off for x-ray diffraction to provide information of where 2-EP substrate in recognized within the structure.

Intellectual Merit and Impact

Studies concerning conjugated polymer syntheses via enzymatic influence remain a novel process. Up till now, only glycosidic hydrolases have been shown to promote this type of "green" chemistry; whether this is unique to this family of enzymes or holds merit in others has yet to be discovered. Nonetheless, the use of proteins to catalyze the synthesis of conjugated polymers represents a significant advance in the adaptation of current mechanisms as well as in the development of newer syntheses null of organic solvents and the use of toxic, transition metal catalysts. Furthermore, development and understanding of these mechanisms may traverse the factions of chemistry and afford collaboration for advances in fields such as photovoltaics and drug delivery systems.

REFERENCES

1 Romero-García, J.; Ledezma-Pérez, A.; Martínez-Cartagena, M.; Alvarado-Canché, C.; Jiménez-Cárdenas, P.; De-León, A.; Gallardo-Vega, C. Radical Addition Polymerization: Enzymatic Template-Free Synthesis of Conjugated Polymers and Their Nanostructure Fabrication. *Methods in Enzymology* **2019**, 321–337.

2 von Hauff, E. The Role of Molecular Structure and Conformation in Polymer Electronics. *Semiconductors and Semimetals* **2011**, 231–260.

3 Jadoun, S.; Riaz, U. Conjugated Polymer Light-Emitting Diodes. *Polymers for Light-Emitting Devices and Displays* **2020**, 77–98.

4 Repenko, T.; Rix, A.; Ludwanowski, S.; Go, D.; Kiessling, F.; Lederle, W.; Kuehne, A. J. Bio-Degradable Highly Fluorescent Conjugated Polymer Nanoparticles for Bio-Medical Imaging Applications. *Nature Communications* **2017**, *8* (1).

5 Chen, H.; Cai, G.; Guo, A.; Zhao, Z.; Kuang, J.; Zheng, L.; Zhao, L.; Chen, J.; Guo, Y.; Liu, Y. Low Band Gap Donor–Acceptor Conjugated Polymers with Indanone-Condensed Thiadiazolo[3,4-*g*]Quinoxaline Acceptors. *Macromolecules* **2019**, *52* (16), 6149–6159.

6 Guimard, N. K.; Gomez, N.; Schmidt, C. E. Conducting Polymers in Biomedical Engineering. *Progress in Polymer Science* **2007**, *32* (8-9), 876–921.

7 Jiang, K.; Zhang, L.; Zhao, Y.; Lin, J.; Chen, M. Palladium-Catalyzed Cross-Coupling Polymerization: A New Access to Cross-Conjugated Polymers with Modifiable Structure and Tunable Optical/Conductive Properties. *Macromolecules* **2018**, *51* (23), 9662–9668.

8 Huang, L.; Wu, S.; Qu, Y.; Geng, Y.; Wang, F. Grignard Metathesis Chain-Growth Polymerization for Polyfluorenes. *Macromolecules* **2008**, *41* (22), 8944–8947.

9 Kobayashi, S. Enzymatic Polymerization: A New Method of Polymer Synthesis. *Journal of Polymer Science Part A: Polymer Chemistry* **1999**, *37* (16), 3041–3056.

10 Shoda, S.-ichiro; Uyama, H.; Kadokawa, J.-ichi; Kimura, S.; Kobayashi, S. Enzymes as Green Catalysts for Precision Macromolecular Synthesis. *Chemical Reviews* **2016**, *116* (4), 2307–2413.

11 Ohmae, M.; Fujikawa, S.-I.; Ochiai, H.; Kobayashi, S. Enzyme-Catalyzed Synthesis of Natural and Unnatural Polysaccharides. *Journal of Polymer Science Part A: Polymer Chemistry* **2006**, *44* (17), 5014–5027.

12 Irazoki, O.; Hernandez, S. B.; Cava, F. Peptidoglycan Muropeptides: Release, Perception, and Functions as Signaling Molecules. *Frontiers in Microbiology* **2019**, *10*.

13 Fodor, C.; Gajewska, B.; Rifaie-Graham, O.; Apebende, E. A.; Pollard, J.; Bruns, N. Laccase-Catalyzed Controlled Radical Polymerization of N-Vinylimidazole. *Polymer Chemistry* **2016**, *7* (43), 6617–6625.

14 Nash, J. A.; Ballard, T. N.; Weaver, T. E.; Akinbi, H. T. The Peptidoglycan-Degrading Property of Lysozyme Is Not Required for Bactericidal Activity in Vivo. *The Journal of Immunology* **2006**, *177* (1), 519–526.

15 Blake, C. C.; Koenig, D. F.; Mair, G. A.; North, A. C.; Phillips, D. C.; Sarma, V. R. Structure of Hen Egg-White Lysozyme: A Three-Dimensional Fourier Synthesis at 2 Å Resolution. *Nature* **1965**, *206* (4986), 757–761.

16 Matthews, B. W.; Remington, S. J.; Grütter, M. G.; Anderson, W. F. Relation between Hen Egg White Lysozyme and Bacteriophage T4 Lysozyme: Evolutionary Implications. *Journal of Molecular Biology* **1981**, *147* (4), 545–558.

17 Meadows, D. H.; Markley, J. L.; Cohen, J. S.; Jardetzky, O. Nuclear Magnetic Resonance Studies of the Structure and Binding Sites of Enzymes. I. Histidine Residues. *Proceedings of the National Academy of Sciences* **1967**, *58* (4), 1307–1313.

18 Schwalbe, H. A Refined Solution Structure of Hen Lysozyme Determined Using Residual Dipolar Coupling Data. *Protein Science* **2001**, *10* (4), 677–688.

19 Baase, W. A.; Liu, L.; Tronrud, D. E.; Matthews, B. W. Lessons from the Lysozyme of Phage T4. *Protein Science* **2010**, *19* (4), 631–641.

20 Jungbauer, A.; Hahn, R. Chapter 22 Ion-Exchange Chromatography. *Methods in Enzymology* **2009**, 349–371.

21 Lucy, C. A. Evolution of Ion-Exchange: From Moses to the Manhattan Project to Modern Times. *Journal of Chromatography A* **2003**, *1000* (1-2), 711–724.

22 Block, H.; Maertens, B.; Spriestersbach, A.; Brinker, N.; Kubicek, J.; Fabis, R.; Labahn, J.; Schäfer, F. Chapter 27 Immobilized-Metal Affinity Chromatography (Imac). *Methods in Enzymology* **2009**, 439–473.

23 Falke, J. J.; Corbin, J. A. Affinity Tags for Protein Purification. *Encyclopedia of Biological Chemistry* **2013**, 61–65.

24 Wohlkönig, A.; Huet, J.; Looze, Y.; Wintjens, R. Structural Relationships in the Lysozyme Superfamily: Significant Evidence for Glycoside Hydrolase Signature Motifs. *PLoS ONE* **2010**, *5* (11).

25 Vedadi, M.; Arrowsmith, C. H.; Allali-Hassani, A.; Senisterra, G.; Wasney, G. A. Biophysical Characterization of Recombinant Proteins: A Key to Higher Structural Genomics Success. *Journal of Structural Biology* **2010**, *172* (1), 107–119.

26 Ziarek, J. J.; Peterson, F. C.; Lytle, B. L.; Volkman, B. F. Binding Site Identification and Structure Determination of Protein–Ligand Complexes by NMR. *Methods in Enzymology* **2011**, 241–275.

27 Williamson, M. P. Using Chemical Shift Perturbation to Characterize Ligand Binding. *Progress in Nuclear Magnetic Resonance Spectroscopy* **2013**, *73*, 1–16.

28 Concepcion, J.; Witte, K.; Wartchow, C.; Choo, S.; Yao, D.; Persson, H.; Wei, J.; Li, P.; Heidecker, B.; Ma, W.; Varma, R.; Zhao, L.-S.; Perillat, D.; Carricato, G.;

Recknor, M.; Du, K.; Ho, H.; Ellis, T.; Gamez, J.; Howes, M.; Phi-Wilson, J.; Lockard, S.; Zuk, R.; Tan, H. Label-Free Detection of Biomolecular Interactions Using BioLayer Interferometry for Kinetic Characterization. *Combinatorial Chemistry & High Throughput Screening* **2009**, *12* (8), 791–800.

29 Duff, Jr., M. R.; Grubbs, J.; Howell, E. E. Isothermal Titration Calorimetry for Measuring Macromolecule-Ligand Affinity. *Journal of Visualized Experiments* **2011**, No. 55.

30 McIntosh, L. P.; Wand, A. J.; Lowry, D. F.; Redfield, A. G.; Dahlquist, F. W. Assignment of the Backbone Proton and Nitrogen-15 NMR Resonances of Bacteriophage T4 Lysozyme. *Biochemistry* **1990**, *29* (27), 6341–6362.

31 Parry, R. M.; Chandan, R. C.; Shahani, K. M. A Rapid and Sensitive Assay of Muramidase. *Experimental Biology and Medicine* **1965**, *119* (2), 384–386.

32 Robert, F.; Pelletier, J. Exploring the Impact of Single-Nucleotide Polymorphisms on Translation. *Frontiers in Genetics* **2018**, *9*.

33 Morris, D. L.; Leeper, T. C.; Ziegler, C. J. Inhibition of Lysozyme's Polymerization Activity Using a Polymer Structural Mimic. *Polymer Chemistry* **2018**, *9* (27), 3705–3708.

34 Cooper, D. R.; Porebski, P. J.; Chruszcz, M.; Minor, W. X-Ray Crystallography: Assessment and Validation of Protein–Small Molecule Complexes for Drug Discovery. *Expert Opinion on Drug Discovery* **2011**, *6* (8), 771–782.

35 Matthews, B. W.; Remington, S. J. The Three-Dimensional Structure of the Lysozyme from Bacteriophage T4. *Proceedings of the National Academy of Sciences* **1974**, *71* (10), 4178–4182.

36 McPherson, A. *Introduction to Macromolecular Crystallography*; Wiley: Hoboken, NJ, 2009; pp 19–49.

37 Rhodes, G.; Rhodes, G. *Crystallography Made Crystal Clear*; Elsevier: Amsterdam, 2006; pp 31–48.

38 Weaver, L. H.; Matthews, B. W. Structure of Bacteriophage T4 Lysozyme Refined at 1.7 Å Resolution. *Journal of Molecular Biology* **1987**, *193* (1), 189–199.

39 Kuroki, R.; Weaver, L. H.; Matthews, B. W. Structural Basis of the Conversion of T4 Lysozyme into a Transglycosidase by Reengineering the Active Site. *Proceedings of the National Academy of Sciences* **1999**, *96* (16), 8949–8954.

40 Plasmid Cloning Using Restriction Enzyme Digest (aka Subcloning) protocol. *Addgene*. https://www.addgene.org/protocols/subcloning/.

41 DNA Ligation protocol. *Addgene.* https://www.addgene.org/protocols/dna-ligation/.

42 PrimerX Bioinformatics: Automated design for mutagenic primers for site-directed mutagenesis. *PrimerX*. https://www.bioinformatics.org/primerx/.

APPENDIX A

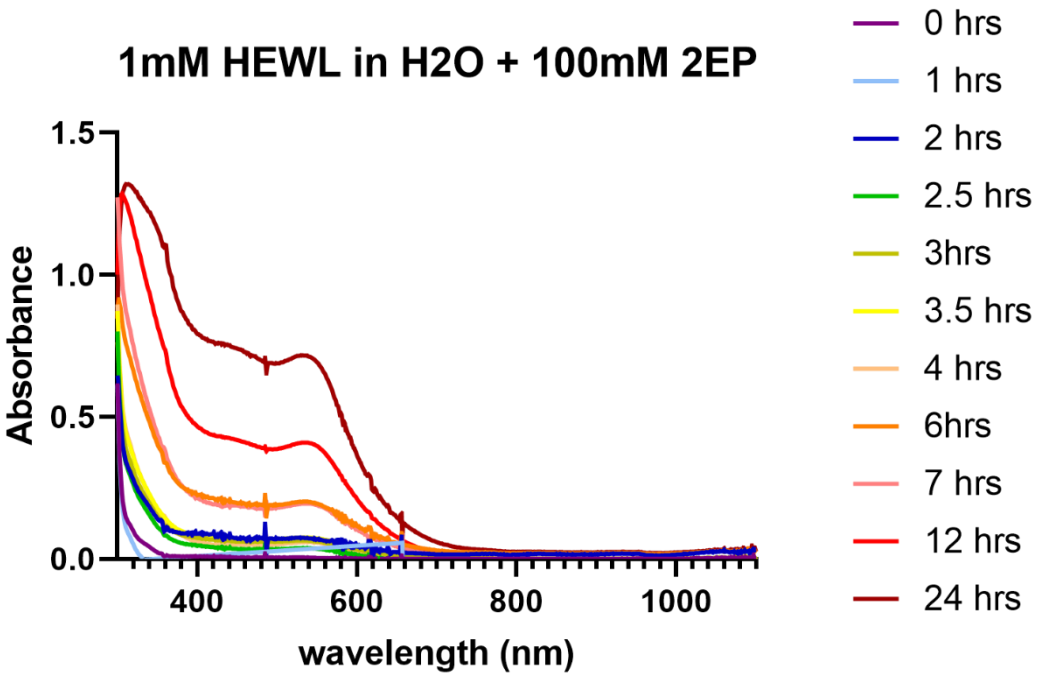

Appendix A.1. Hen egg-white lysozyme (HEWL) ability to polymerize 2-EP to form a conjugated polymer. Polymer accumulation was determined to occur around 541 nm; the value corresponding to this at each hourly interval were plotted and graphed to assess rate of polymerization. A sigmoidal curve can be seen over time, often associated with cooperatively allosteric enzymes, with increasing substrate concentration of 2-EP.

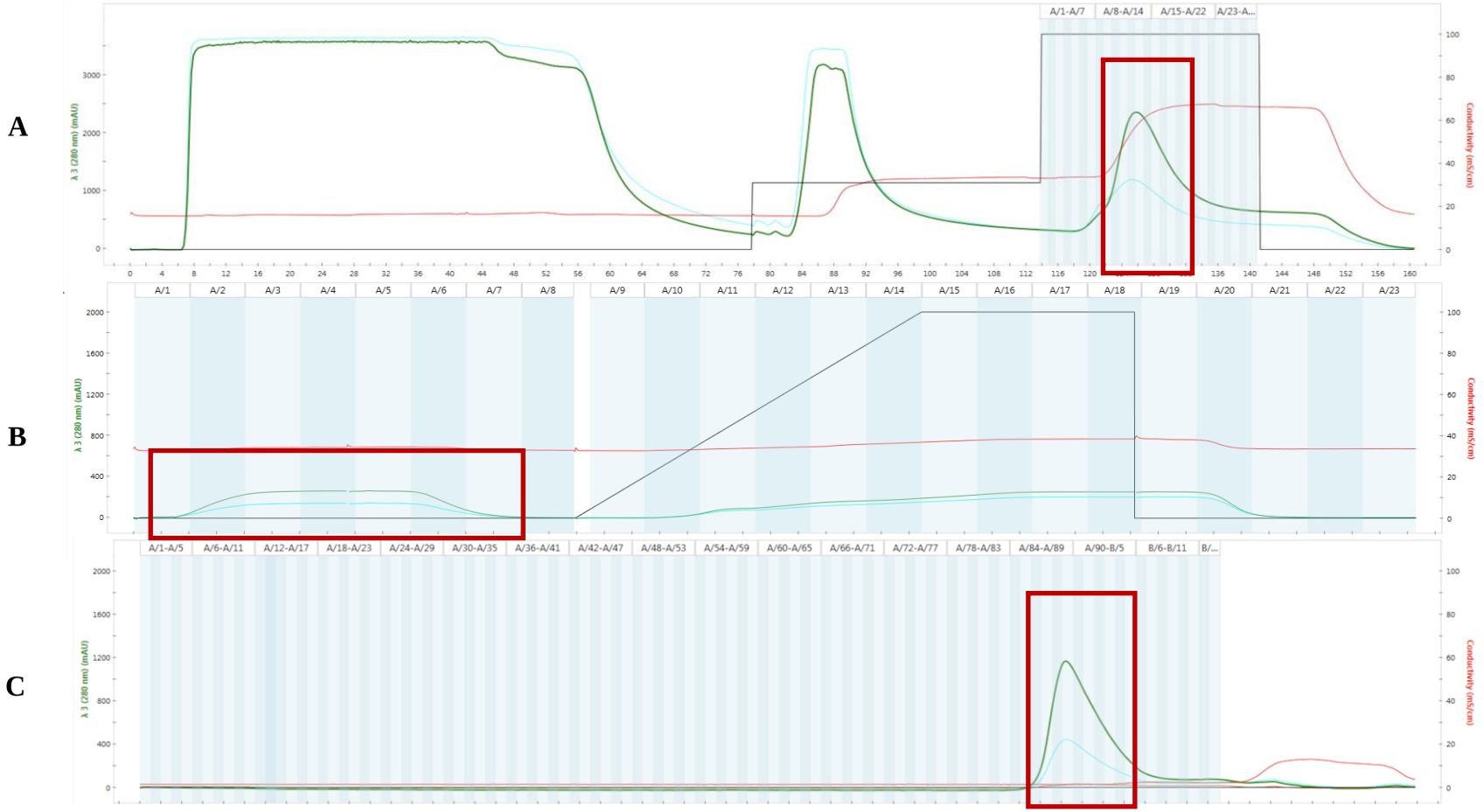

Appendix A.2. Purification of T4L proteins using IMAC. Wavelengths are as described as follows: λ_{255} (cyan), λ_{280} (green), conductivity (red), and buffer gradient (black). As depicted from each chromatogram purification strategy was successful in isolating protein of interest (a), separating cleaved protein from the histidine tag using TEV protease (b), and providing relatively pure protein following SEC refinement (c). Red boxes indicate the target protein, T4L after each purification step.

T4L WT — 0.776 mM stock to X mM HEWL — 5mM stock to 0.125 mM

2-EP / T4L	60 mM 1.5uL	60 mM 1.5uL	90 mM 2.25uL	90 mM 2.25uL	100 mM 2.5uL	100 mM 2.5uL	120 mM 3.0uL	120 mM 3.0uL	150 mM 3.75uL	150 mM 3.75uL	180 mM 4.5uL	180 mM 4.5uL
0.0mM T4L (HEWL)	5.6 H 217.9	--------- 223.5	5.6 H 217.15	--------- 222.75	5.6 H 216.9	---------- 222.5	5.6 H 216.4	------- 222	5.6 H 215.65	------- 221.25	5.6 H 214.9	------- 220.50
0.125 mM T4L	36.24 T 187.26	------- 223.5	36.24 T 186.51	--------- 222.75	36.24 T 186.26	---------- 222.5	36.24 T 185.76	------- 222	36.24 T 185.01	------- 221.25	36.24 T 184.26	------- 220.50
0.250 mM T4L	72.48 T 151.02	------- 223.5	72.48 T 150.27	--------- 222.75	72.48 T 150.02	---------- 222.5	72.48 T 149.52	------- 222	72.48 T 148.77	------- 221.25	72.48 T 148.02	------- 220.50
0.500 mM T4L	145.0 T 78.50	------- 223.5	145.0 T 77.75	--------- 222.75	145.0 T 77.5	---------- 222.5	145.0 T 77.0	------- 222	145.0 T 76.25	------- 221.25	145.0 T 75.5	------- 220.50

Appendix A.3. Concentrations of T4L and HEWL used in preliminary kinetic assays. 2-EP varied along the top ranging from 60 mM to 180 mM whereas protein and their respective concentrations varied top down. HEWL has shown to perform this polymerization via Appendix A.1 and served as the control for this experiment. Preparation of each reaction is further described in Appendix C.

Appendix A.4. Crystallography conditions for growing T4L crystals.

PDB	Buffer Contents	pH	Additives	Cryo	Type?	Temp
1C69, 1C6A, 1C6B	1.8-2.2 M NAH2/K2HPO4	6.9-7.1	50 MM BME AND/OR 50 MM HEDS		HANGING	4 °C
1D9W	2.1-M PHOSPHATE	6.5	10 MM BME AND/OR 20 MM OXBME		HANGING	5 °C
2F32, 2F2Q, 1T8A	1.8 M MIXED POTASSIUM AND SODIUM PHOSPHATE, 0.2 M ETHYL GUANIDINIUM CHLORIDE	6.5			HANGING	4 °C
3F8V, 3F91, 3F80, 3FAD	2 M NA/K PHOSPHATE	6.3			HANGING	4 °C
1T97, 201L,	30% POLY-ETHYLENE GLYCOL 3400, 100MM HEPES BUFFER, 200MM AMMONIUM ACETATE	7.5			HANGING	4 °C
1BIA	60% SATURATED AMMONIUM SULPHATE, 100 MM BIS-TRIS PROPANE	8.5			HANGING	4 °C
1C1K	100 MM NA CACODYLATE, 200 MM NH4 ACETATE, 50 MM (NH4)2SO4, 10 - 14% PEG 3350 GRADIENT, 20% ETHYLENE GLYCOL	6.5			HANGING	4 °C
1EPY	12-16% PEG 8000, 10% ISOPROPANOL, SODIUM CHLORIDE, HEPES, 0.002 M COBALT CHLORIDE	7.0			HANGING	4 °C
1G1V	2.1 M NAH2/K2HPO4	7.1	50 MM HEDS		HANGING	4 °C
1JQU	30% PEG 4000, PIPES BUFFER, 0.2 M LISO4	7.0, 6.5			HANGING	4 °C
1JTM	50 MM TRIS-GLYCINE, 20% PEG 8000, 10% ISOPROPANOL	7.0			HANGING	5 °C
1JTN	50M TRIS-GLYCINE, 200 MM LISULFATE, 18% PEG 4000	6.8			HANGING	5 °C
1P2L	25% PEG 4000, 50 MM PHOSPHATE BUFFER, 0.2 MM AMMONIUM ACETATE, 20% ISOPROPANOL	5.5			HANGING	5 °C
1P37	2 M SODIUM/POTASSIUM PHOSPHATE, 550 MM NACL	5.6	40 MM BME		HANGING	4 °C
220L, 222L	PROTEIN 10-20 MG/ML IN A BUFFER CONTAINING 0.1 M NA2PO4 pH: 6.6, 0.55 M NACL WAS DILUTED 1/2 WITH A WELL SOLUTION CONTAINING 1.8-2.2M NA/KPO4, pH: 6.3-7.1	7.0			HANGING	4 °C
223L, 225L	PROTEIN 10-20 MG/ML IN A BUFFER CONTAINING 0.1 M NA2PO4 pH: 6.6, 0.55 M NACL WAS DILUTED 1/2 WITH A WELL SOLUTION CONTAINING 1.8-2.2M NA/KPO4, pH: 6.3-7.1	7.0	? MM BME	BENZENE VAPOR; P-XYLENE VAPOR	HANGING	4 °C
231L, 232L	0.1 M NA2PO4 pH: 6.6, 0.55 M NACL. DILUTED BY 1/2 WITH 1.8 M NA/KPO4 pH: 6.9	7.0			HANGING	4 °C
2HUL	2.0 M AMMONIUM SULFATE, 0.1 M NA CACODYLATE pH: 6.7, 0.2 M NACL	6.7			HANGING	4 °C
2HUK	20% PEG 8000, 0.1 M NA CACODYLATE, pH: 6.5, 0.2 M AMMONIUM ACETATE	6.5			HANGING	2 °C

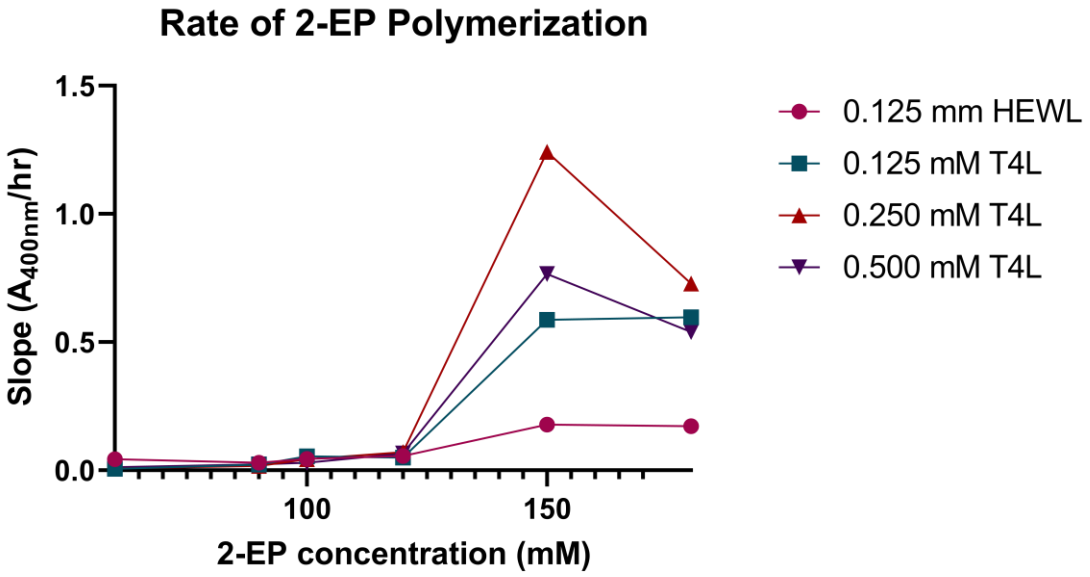

Appendix A.5. Rate of polymer formation in relation to 2-EP concentration. Line colors represent varied concentrations of wild-type T4L, with HEWL serving as a positive control. From these data, upper concentrations of both T4L and 2-EP yield a higher rate of polymer formation and hinder the ability to assess rate effectively. Additionally, these higher concentrations showed initial precipitate which does not support quality science.

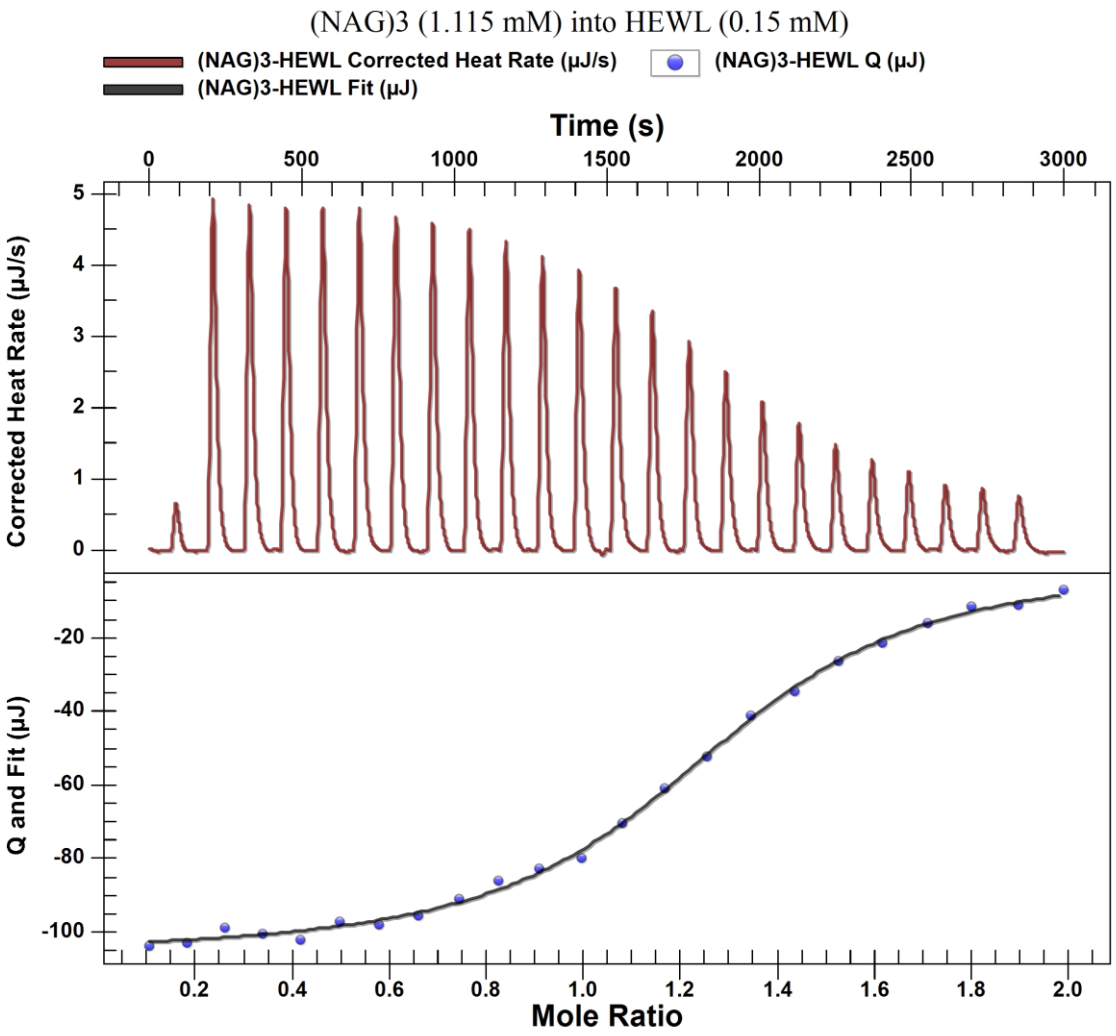

Appendix A.6. Titration of 1.115 mM $(NAG)_3$ into 0.15 mM HEWL. The corrected heat rate was observed as it related to time of each 2 µL titration of $(NAG)_3$ into 300 µL of HEWL. Buffer conditions were in 18 MΩ water. Condition was run as a preliminary run to assess instrument function and software.

Appendix A.7. Comparison of various biophysical methods.

Biophysical Screening Method	Throughput	Suitable instruments (examples)	Protein requirement	Advantages	Limitations
Fluorescence assay (lysozyme activity assay)	96-well format 96-well format	Synergy H1™ from BioTek iD5 microplate reader from SpectraMax®	50 µL of purified protein for serial dilution	- Independent of protein function - Relatively high throughput	- Sensitive to light/ fluorescence
2-ethynylpyridine assay (polymer kinetics assay)	96-well format	iD5 microplate reader from SpectraMax®	Variable	- Independent of protein function - Relatively high throughput	- High amount of protein requirement - Slow polymerization reaction (≥8 hours)
Nuclear magnetic resonance (NMR)	Relatively low	Ascend™ 600 MHz from Bruker Ascend™ 400 MHz from Bruker	≥ 50 µM sample for proteins < 35 kDa	- Independent of protein function - Provides structural data via data acquisition - Suitable for assessing folding/ unfolding and ligand binding - Allows for isotopic labeling of amino acid residues, ^{15}N and ^{13}C - Preserves sample integrity, non-destructive	- Structure determination for larger proteins (>35 kDa) - High protein concentration requirement - Relatively low throughput
Isothermal titration calorimetry (ITC)	Relatively low	Nano ITC from TAInstruments	Low µM to high low mM range	- Independent of protein function - K_D determination for macromolecule interaction - Provides thermodynamic binding parameters	- High protein concentration requirement - Relatively low throughput - Inability to determine on-and-off rates of macromolecule interactions
Biolayer interferometry (BLI)	Relatively high	OctetRED 96c from FortéBio	10 pM to 1 mM range (OctetRED 96c)	- Real-time on-and-off rates of macromolecule interactions - K_D determination for macromolecule interaction	- Requires protein or ligand immobilization - Approximately 100-fold lower sensitivity of detection (difficult to assess binding of small molecules)
X-ray crystallography (XRC)	24-well format	D8-Advance™ from Bruker*	≥ 20 mg/mL protein sample	- Provides structural data via crystal diffraction - Useful for structure determination of larger proteins (>35 kDa)	- High protein concentration requirement - Optimization of crystal growth conditions ∴ must be able to be crystallized

*Performed at UGA x-ray crystallography core.

Appendix A.8. IDTdna primers for site-directed mutagenesis of *bacteriophage T4 lysozyme*.

Primer	Amount of Oligo (mg) [a]	T_M (°C) [b]	Sequence	Intended rationale for mutation
R31G (Forward)	0.27 mg	55.2	5′ –GTTACGTATAGATGAAGGTCTTAGACTTAAAATC– 3′	Revert to glycine (G) to promote T4L sequence homology
R31G (Reverse)	0.29 mg	55.2	5′ –GATTTTAAGTCTAAGACCTTCATCTCTACGTAAC– 3′	Revert to glycine (G) to promote T4L sequence homology
I156R (Forward)	0.25 mg	55.7	5′ –CTTAGCTAAAAGTAGATGGTATAATCAAACACC– 3′	Revert to arginine (R) to promote T4L sequence homology
I156R (Reverse)	0.19 mg	55.7	5′ –GGTGTTTGATTATACCATCTACTTTTAGCTAAG– 3′	Revert to arginine (R) to promote T4L sequence homology
E30Q (Forward)	0.20 mg	55.1	5′ –GAAATGTTACGTATAGATCAAGGTCTTAGAC– 3′	Proposed active site residue, E30
E30Q (Reverse)	0.23 mg	55.1	5′ –GTCTAAGACCTTGATCTATACGTAACATTTC– 3′	Proposed active site residue, E30
D39A (Forward)	0.21 mg	56.9	5′ –GACTTAAAATCTATAAAGCCACAGAAGGCT– 3′	Proposed active site residue, D39
D39A (Reverse)	0.21 mg	56.9	5′ –AGCCTTCTGTGGCTTTATAGATTTTAAGTC– 3′	Proposed active site residue, D39
del_C 1.1 (Forward)	0.17 mg	60.5	5′ –CATCACCATCACCATACCATCACCATGAG– 3′	Invoke a frameshift to reduce 10-histidine tag to 6-histidine tag
del_C 1.1 (Reverse)	0.20 mg	60.5	5′ –CTCATGGTGATGGTATGGTGATGGTGATG– 3′	Invoke a frameshift to reduce 10-histidine tag to 6-histidine tag
ins_C 1.2 (Forward)	0.18 mg	59.8	5′ –CATACCATCACCATCGAGAACCTGTACTTC– 3′	Re-alignment of frameshift via 1.1 primer pair
ins_C 1.2 (Reverse)	0.16 mg	59.8	5′ –GAAGTACAGGTTCTCGATGGTGATGGTATG– 3′	Re-alignment of frameshift via 1.1 primer pair
ins_C 2.1 (Forward) [c]	0.17 mg	61.4	5′ –CATCACCATCACCATCGAGAACCTGTACTTC– 3′	Invoke a frameshift to reduce 10-histidine tag to 6-histidine tag
ins_C 2.1 (Reverse) [c]	0.23 mg	61.4	5′ –GAAGTACAGGTTCTCGATGGTGATGGTGATG– 3′	Invoke a frameshift to reduce 10-histidine tag to 6-histidine tag
del_C 2.2 (Forward) [c]	0.12 mg	59.4	5′ –CACCATCACCATACCATCACCATCG– 3′	Re-alignment of frameshift via 2.1 primer pair
del_C 2.2 (Reverse) [c]	0.17 mg	59.4	5′ –CGATGGTGATGGTATGGTGATGGTG– 3′	Re-alignment of frameshift via 2.1 primer pair

[a] primers were diluted to $1\ \mu g/\mu L$

[b] T_M values provided per IDTdna; PCR conditions use (T_M - 5 °C), and vary per reaction

[c] primer never reconstituted; ordered as alternative to initial frameshift primers (*1.1, 1.2*)

APPENDIX B

PURIFICATION PROTOCOL FOR HIS-TAGGED T4L PROTEINS

WILLIAM D. TURNER

Optimal Cell Line: *E. coli* BL-21 (DE3) pLysS

Plasmid: T4p123 in pBAD/HIS-A vector

Promoter: PBAD-Forward

Antibiotic resistance: Ampicillin

Induction: 0.1% (w/v) L-(+)-Arabinose @ OD_{600} 0.4-0.6

Extinction Coefficient: 25440

Molecular Weight: 18.7 kDa

pI: 9.76

Buffer Conditions: 40 mM Potassium Phosphate, 200 mM Potassium Chloride, pH 8.0

Room Temperature Stable / 4°C Preferred

Withstands Freeze-thaw Cycles

Withstands De-Salting into Water

TRANSFORMATION

Required Materials.

Bucket with ice

1 mL stock of SOC media

T4L plasmid

BL-21 (DE3) pLysS single shot cells (~50 µL)

2 – Ampicillin LB/Agar plates

1 – Kanamycin LB/agar plate

Method.

1 Place BL-21 (DE3) pLysS single shot ampule and plasmid in ice bucket to thaw

2 Place SOC media on benchtop from refrigerator to warm up

3 Label the bottom of each plate with the following information: [plasmid_cell line_date_initials] and place all three LB/Agar plates in incubator at 37°C

4 Once cells and plasmid are thawed, **pipet 2 µL of plasmid directly into 20 µL of cells** and place back on ice for 30 minutes.

5 Heat-shock for **42 seconds at 42°C**

6 Place back on ice for an additional 5 minutes

7 Add 480 µL of SOC media to cells and place in 37°C shaker @ 260 rpm for 45 minutes to an hour

8 Pipet 50 µL and 100 µL of incubated cells onto either ampicillin plate, 100 µL onto the kanamycin plate. Spread evenly on each plate using either sterile glass or plastic spreaders

9 Incubate at 37° overnight

10 Parafilm and store in bottom bin of Leeper Lab refrigerator. **Shelf life: 1-2 weeks**

SMALL INOCULUM

Required Materials.

2 – 250 mL Erlenmeyer flasks (autoclaved) with 50 mL of sterile 2X-YT media in each

1 – 1 mL Ampicillin stock

Transformation plate

Sterile, inoculating loop

Method.

1 Pull transformation plates and ensure plates are in date and have no suspicious growth

2 Using sterile loop, swab 2-3 isolated colonies from the plate and vigorously stir into flask. Repeat this for the second flask

3 Once thawed, add 50 µL of ampicillin stock to each flask ***Mark with a single, black dot to indicate prior use. After two uses, discard remaining antibiotic***

4 Cover top of flask with foil and place in shaker at 37^{o}C overnight

LARGE INOCULUM

Required Materials.

2 – 2600 mL Fernbach flasks (autoclaved) with either 950 mL of sterile 2X-YT or filter-sterilized M9 minimal media

2 – Incubated cultures from the small inoculum

Spectrophotometer

Plastic cuvettes

2 – 1.0 g of L-(+)-Arabinose weighed out

2 – 1 mL Ampicillin stocks

Method.

1 Turn on spectrophotometer

2 Spike 950 mL of selected media with 1 mL of ampicillin stock solution

3 Reserve 1 mL of this media as a blank

4 Pull small inoculums from the shaker, pour entire contents into either Fernbach flask, cover with foil, and shake to homogenize

5 Pipet 1 mL into cuvette, record OD_{600}. Induction **OD_{600} = 0.4-0.6 mAU**

If OD_{600} is below 0.4, shake at 37°C for 30-minute intervals, taking OD_{600} readings at each interval until absorbance is 0.4-0.6 mAU.

If OD_{600} is within range, move to step 6.

6 Reserve 200 µL of non-induced sample and place in a 1.7 mL Eppendorf tube

7 Induce with L-(+)-arabinose to a ratio of 0.1% (w/v) **0.1% (w/v) is equivalent to 1 g of L-(+)-arabinose per 1L media *Adjust amount accordingly to amount of media use***

8 Label flask and secure non-induced sample to the Fernbach flask using label tape

9 Replace in shaker and reduce temperature to 22°C

LARGE INOCULUM CENTRIFUGE PROTOCOL

Required Materials.

Thermo Scientific Sorvall Lynx 4000 Superspeed Floor Centrifuge

F10-6X500Y Rotor from cold room

500 mL centrifuge bottles with screw caps

2 – Incubated cultures from the large inoculum

Method.

1 Turn on centrifuge and place rotor inside unit, screwing lid onto rotor, then securing top screw into centrifuge.

2 'Quick-temp' the centrifuge by setting rotor on screen. Start spin then immediately stop. This kickstarts the compressor.

3 Set parameters to 10,000 RPM at 15 minutes, 4^{o}C

4 Reserve 200 µL of induced sample and place in a 1.7 mL Eppendorf tube

5 Pour large inoculum culture into centrifuge bottles. Volume should be around 2/3 the height of bottle.

6 Balance filled bottles against each other using Harvard balance.

7 Place balanced bottles across from one another to balance rotor

8 Secure the lid to rotor

9 Secure the rotor to centrifuge

10 Confirm rotor and spin settings

11 Start and step back

WARNING! ROTOR IS SUSCEPTIBLE TO FAILURE DURING ACCELERATION AND DECELERATION

12 Pour off clear supernatant and **repeat steps 5-12 until all culture has been centrifuged**. Store pellets in -20^{o}C freezer

13 Bleach supernatant and culture bottles for an hour minimum

14 Bleach work area and balance

BUFFERS

Required Materials.

1 L or 2 L graduated cylinder

2.5 L beaker with stir bar

Potassium phosphate, dibasic

Potassium phosphate, monobasic

Potassium chloride

Imidazole, 99%

6M Hydrochloric acid (HCl)

6M Potassium hydroxide (KOH)

Digital analytical balance

Stir plate

pH meter

Vacuum filter apparatus with appropriate filter paper

Method.

1 Place 500 mL of 18 MΩ deionized water in beaker with stir bar. Place beaker on stir plate

2 Weigh ingredients for respective buffer using analytical balance

3 Dissolve ingredients into water

4 Adjust pH to 8.0 using pH meter and appropriate acid or base

5 Pour into appropriate graduated cylinder and bring up to volume using 18 MΩ DI H_2O

6 Vacuum filter and degas buffer

7 Store Buffer A, Buffer B, and SEC buffer in clean, autoclaved 1L glass screw cap bottle

Dialysis buffer may be stored in a 2.5 L Nalgene beaker covered with plastic wrap in either the cold room or NGC deli-fridge

8 Apply appropriate label with product name, contents, pH, your name, and date

Example: T4L-HIS Buffer A – 40 mM Potassium Phosphate, 200 mM Potassium Chloride, 20 mM imidazole, pH: 8 – WDT 5/3/22

BUFFER COMPONENTS (IDENTICAL TO paIVY BUFFERS)

Buffer Name	Running Buffer "Buffer A"	Elution Buffer "Buffer B"	SEC Buffer	Dialysis Buffer
Volume	1 Liter	1 Liter	1 Liter	2 Liters
pH	8.0	8.0	8.0	8.0
Dibasic Potassium Phosphate, K_2HPO_4 (Anhydrous)	20 mM 3.846 g	20 mM 3.846 g	20 mM 3.846 g	20 mM 7.692 g
Monobasic Potassium Phosphate, KH_2PO_4 (Anhydrous)	20 mM 2.722 g	20 mM 2.722 g	20 mM 2.722 g	20 mM 5.444 g
Potassium Chloride, KCl	200 mM 14.910 g	200 mM 14.910 g	200 mM 14.910 g	200 mM 29.820 g
Imidazole	20 mM 1.362 g	400 mM 27.232 g		

HOMOGENIZATION

Required Materials.

500 mL centrifuge bottles with pellets from large inoculum centrifugation

25 mL Buffer A

60 mL homogenizer with plastic plunger

Ice bucket with ice

Method

1 Pour 25 mL Buffer A into one centrifuge bottle with pellet. Using a glass stir rod and gently agitate pellet until completely loosened into the buffer

2 Pour off contents of the bottle into the next centrifuge bottle with pellet

3 Repeat steps 1-2 until all pellets have been loosened

4 Pour contents into homogenizer and place in ice

5 Use plunger with an up/down and twisting motion to homogenize cells into buffer A. Product should be a uniform, creamy, light tan solution

FRENCH PRESS

CAUTION! VERY DANGEROUS. USES A COMBINATION OF HIGH PRESSURE FROM AN OPEN HYDRAULIC PRESS AND 10 kg STEEL CELL. SEVERE INJURY MAY OCCUR WITH IMPROPER USE. SAFETY BUDDY SHOULD BE PRESENT WHEN OPERATING!

Required Materials.

Hydraulic French press

- French press cell with T-bar plunger

Homogenized cell culture

250 mL beaker with ice

Bucket with ice

Method.

1 Ensure French press machine is set to "down" and "pause". Turn on machine

2 Lubricate rubber on plunger with petroleum jelly and assemble cell body with T-bar plunger to "MAX FILL" line

3 Place upside down onto cell stand

4 Assemble the base of cell with outlet nozzle and flow restrictor screw **tightened**

5 Pour homogenized sample into cell body. Make sure to leave about 3 cm of room for the cell base

6 Place cell base onto cell body and invert to right side up

7 Place assembled cell into press with the T-bar above the T bar plunger notches. Cell should be positioned with the plastic button on the cell body in line with the steel screw rod, outlet nozzle facing forward, and flow restrictor screw easily accessed to the left

8 Secure the cell in place using steel cross bar with screw assembly

9 Attach outlet nozzle hose

10 Set to "LOW" and "RUN". Allow pressure to stabilize (~1750 PSI). Make sure cell has not moved from its restraints and that the T-bar has made flush contact with the top plate. You should not see any flow through the outlet hose

11 Set to "HIGH". Allow pressure to stabilize. You should not see flow through the outlet hose

12 Using the small mallet, tap the flow restrictor screw in a counterclockwise fashion until a slow flow is seen in the outlet hose

13 Once the flow has reached the end of the outlet hose, regulate the flow to 1-2 drops per second into a small centrifuge bottle. Contents in the hose should look like a dark tan liquid with cream liquid on top

14 Run until the plunger reaches “STOP”. Set machine to “PAUSE”

15 Set machine to “DOWN” and “RUN”

16 **Repeat steps 3-15 two times**

CRUDE LYSATE CENTRIFUGATION

Required Materials.

Thermo Scientific Sorvall Lynx 4000 Superspeed Floor Centrifuge

F21S 8X50Y centrifuge rotor from cold room

Crude lysate from French press

2 – 30 mL centrifuge bottles

Method.

1 Turn on centrifuge and place rotor inside unit, screwing lid onto rotor, then securing top screw into centrifuge.

2 'Quick-temp' the centrifuge by setting rotor on screen. Start spin then immediately stop. This kickstarts the compressor.

3 Set parameters to 27,000 RPM at 45 minutes, 4^{o}C

4 Balance samples using Harvard balance

5 Place balanced bottles across from one another to balance rotor

6 Fasten bottom screw and top screw to rotor

7 Confirm run conditions and rotor selection

8 Start and step back

WARNING! ROTOR IS SUSCEPTIBLE TO FAILURE DURING ACCELERATION AND DECELERATION

9 After run is complete immediately pour off supernatant into a 50 mL falcon tube

10 Take a 100 µL sample of the supernatant placing it in a 1.7 mL Eppendorf tube. Label 'CRUDE'

11 Inspect pellet. The outside edge of the pellet should be glassy and transparent. This represents cell membrane fragments. As you inspect closer to the center, the color should be tan with a dark bullseye representing heavier bacterial cell fragments

CROMLAB PROGRAM BASICS FOR NGC LIQUID CHROMATOGRAPHY SYSTEM

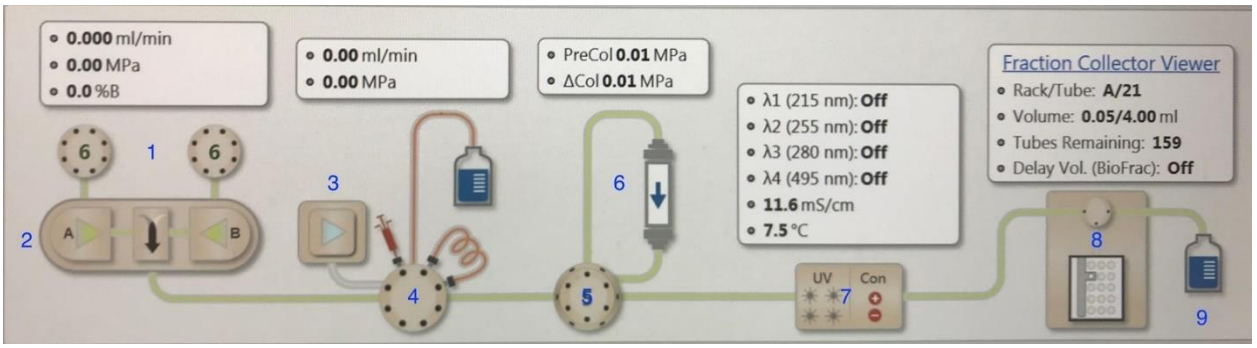

1 System Pump Buffer Selection Icon for Pump A and Pump B

- Allows to change between buffers using valve

2 System Pump Operation Icon

- Allows pump A and B operation. Allows for isocratic or gradient elution functions

3 Sample Pump Operation Icon

- Load and/or Inject Sample

4 Sample Pump Flow Selection Icon

- Changes selection to loop or direct column, inject for sample pump, and system pump

5 Column Selection Icon

- Changes flow to selected column

6 Column Icon

7 UV/Connectivity Icon

- Toggle lamps on/off, zero absorbance readings

8 Fraction Collection Icon

- Set collection tube parameters – type/volume/amount

9 Waste icon

1ST NI-COLUMN (HIS-I) PURIFICATION BY IMMOBILIZED METAL AFFINITY CHROMATOGRAPHY (IMAC)

The purpose of this purification step is to separate our protein from the rest of the bacterial proteins by leveraging the utility of the 6-histidine tag. When the crude lysate flows across the nickel column, the nickel binds T4L which contains a his-tag. Low imidazole concentration running buffer that flows over the column in the next step helps kick off weakly binding proteins. High concentration imidazole in an elution buffer knocks T4L off the nickel column. There are a few important cautionary steps whenever purifying protein on the NGC. First, make sure you do not introduce any air into the system. Introducing air into a column can dry out the column matrix and destroy the column. Second, make sure flow is within operating range for the column you are using. Using a flow rate too high for a column will compress the matrix and destroy the column. Third, ensure that the fraction collector is turned on and is connected to the NGC before loading your protein. If the fraction collector is not communicating with the NGC, the entire system must be restarted. Finally, once the protein is loaded, do not zero out the absorbance. This will skew your results.

Required Materials.

NGC Liquid Chromatography System equipped with ChromLab program

T4L Buffer A (see page 8) placed in buffer selector 3A

T4L Buffer B (see page 8) placed in buffer selector 3B

Centrifuged crude lysate

3 – 50 mL falcon tubes labelled 1) buffer A 2) flow through 3) peak fractions

Methods.

1 Equilibrate the Ni-column.

i) Set column selection icon to slot 1
ii) Run DI water (system pump buffer selector slot 2) at 5 mL/min for 25 mL
iii) Run buffer B (system pump buffer selector slot 3 100%B) @ 5mL/min 25 mL
iv) Run buffer A (system pump buffer selector slot 3 0%B) @5mL/min 25 mL, zeroing out the absorbance under UV/Conn icon within 5 mL of completion
v) Set column selection icon to bypass
vi) Set sample pump flow selection to “Sample pump direct inject, system pump waste.” line on computer diagram should be light blue from the sample pump through the column and into waste.
vii) Using sample pump, direct inject 10 mL buffer A to clear out sample pump.
viii) Turn column selection icon back to position 1

ix) Clear out run

2 Load the CRUDE Lysate

i) Take the empty 50 mL falcon tube labelled "flow through" and place in plastic waste jug with lines in the falcon. The tube should not fall through into the bottom. it should sit on the lid of the waste collector
ii) Determine volume of centrifuged lysate and set injection volume of sample pump
iii) Place falcon tube into clamp by sample pump. Insert brown sample loading tube to the bottom of the falcon
iv) Load sample using sample pump at 5 mL/min. stop pump just before all sample is gone. A large plateau should appear on the chromatogram
v) Add approximately 10 mL buffer A at 5 mL/min to residual crude lysate and run sample pump for ~10 mL to ensure injection of all crude lysate
vi) Remove "flow through" falcon tube from the waste container
vii) Switch sample pump flow selection to "Manual inject loop, system pump to column." Flow line on computer diagram should show a red injection loop and a green line running from the system pump through the column and to waste.

3 Set up Fraction Collection

i) Ensure fraction collector is on, has clean racks in it, and is connected to the system
ii) Click on the blue fraction collector viewer icon and press both "Remove Empty Racks" and "Remove All"
iii) Close out window
iv) Double click on fraction collector to open window. Rack type should be F1 (12-13 mm X 100mm tubes). Start collection from A1 and end at B90. Fraction size should be 2 mL

4 Achieve Adequate Separation

i) Set system pump to 5 mL/min, 0% B, for 25 mL. Start Pump
ii) Turn on fraction collection by double clicking fraction collector and pressing "Collect."
iii) Absorbance line should be near or at baseline after 25 mL run. If not, run 10 mL at a time until the baseline of A280 is less than 50 mAU

5 Elute T4L from the column

i) Under the system pump, choose gradient, initial %B 0%, final %B 100%, 25 mL then click the check box to run final B% for an additional 15 mL
ii) Start flow. A peak should appear around 30%B
iii) At 100%B, you will notice that A280 flattens out around 500 mAU. To establish this is absorbance from the high concentration imidazole, run 15 mL

0%B and watch the absorbance line and the connectivity line. the line shapes should be very similar. A280 should drop down close to zero

6 Finishing up

i) Stop collection
ii) Press “Reset Arm”
iii) Collect fractions from peak in 50 mL falcon labelled “Peak Fractions”
iv) Add 1:1000 EDTA to peak fraction falcon
    - If you collected 16 mL sample, add 16µL EDTA
v) Save run: [protein_media_labelling, if applicable_date_initials]
vi) Close out run and open ‘Analysis’
vii) Deselect every line trace except A280, A255, %B, and Connectivity
viii) Create run report under File
ix) Save in a folder created on desktop

DIALYSIS AND TEV CLEAVAGE

The purpose of this step is to remove excess imidazole from the peak fractions to allow cleavage of the TEV cleavage site [ENLYFQ | G/S] to separate the poly-histidine tag.

Required Materials.

Pooled peak fractions containing 0.5 mM (1:1000 dilution) Disodium EDTA from 0.5 M stock

TEV protease, in-house (2 mg/mL)

3500 MW Snakeskin® dialysis tubing with green tube clamps

2L dialysis buffer (see page 8)

Methods.

1 Soak a strip of 3500 MW Snakeskin® dialysis tubing in dialysis buffer to hydrate dialysis membrane

2 Fold the first end of the dialysis tubing in a "greek key" motif by making one large fold, then folding the large fold in half. clamp the folded membrane with a green clip

3 Using a disposable pipet, transfer the pooled fraction containing EDTA into the dialysis tubing. Clamp the second end of the tubing using the same folding technique. make sure there is an air bubble in the dialysis tubing, allowing the tubing to float in the dialysis buffer.

4 Place dialysis tubing in dialysis buffer for at least 3 hours to reduce the imidazole concentration in the pooled fractions.

5 After initial dialysis, remove the dialyzed protein and add entire shot of 2 mg/mL TEV protease

6 Set on benchtop overnight or in the cold room at 4°C. ***Be mindful, TEV protease cleaves at a slower rate when in colder conditions***

7 After dialysis, transfer the dialyzed protein into a clean 50 mL falcon tube.

2ND NI-COLUMN (HIS-II) PURIFICATION BY IMMOBILIZED METAL AFFINITY CHROMATOGRAPHY (IMAC)

The purpose of this purification step is to further purify your protein by separating the cleaved T4L protein from the TEV, N-terminal his-tag, and any non-specific binding proteins that co-eluted with T4L during the first nickel column. We use a cleave and clear strategy to remove the his-tag from our protein. By running our protein over a nickel column a second time, the flow through will contain T4L and the His tag along with TEV will come off of the column with the elution fraction.

Required Materials.

NGC Liquid Chromatography System equipped with ChromLab program

T4L Buffer A (see page 8) placed in buffer selector 3A

T4L Buffer B (see page 8) placed in buffer selector 3B

Dialyzed T4L with TEV

2 – 50 mL falcon tubes labelled 1) Buffer A 2) HIS II Peak Fraction

Methods.

1 Add imidazole to dialyzed protein.

i) Doping in imidazole to 20 mM will decrease likelihood of T4L sticking to Ni column during the loading phase. This will make your loading peak look like a plateau versus a gradually rising slope.
ii) There is an easy formula: look at how much protein you have (volume). Multiply this number by 20. This is how many MICROLITERS of 1 M imidazole you should add to your protein.
Example: If given 24 mL of protein, 24 x 20 = 480 µL of 1M imidazole

2 Equilibrate the Ni-column

i) Set column selection icon to slot 1
ii) Run DI water (system pump buffer selector slot 2) at 5 mL/min for 25 mL
iii) Run Buffer B (system pump buffer selector slot 3 100%B) @ 5mL/min 25 mL
iv) Run Buffer A (system pump buffer selector slot 3 0%B) @ 5mL/min 25 mL, zeroing out the absorbance under UV/Conn icon within 5 mL of completion
v) Set column selection icon to bypass
vi) Set sample pump flow selection to "Sample pump direct inject, system pump waste." The line on the computer diagram should be light blue from the sample pump through the column and into waste
vii) Using sample pump, direct inject 10 mL Buffer A to clear out sample pump

viii) Turn column selection icon back to position 1
ix) Clear out run

3 Load the T4L and TEV sample

i) Take the empty 50 mL falcon tube labelled “His 2 Peak Fraction” and place in plastic waste jug with lines in the falcon. The tube should not fall through into the bottom. it should sit on the lid of the waste collector.
ii) Determine volume and set injection volume of sample pump.
iii) Place falcon tube into clamp by sample pump. Insert brown sample loading tube to the bottom of the falcon.
iv) Load sample using sample pump at 5 mL/min. stop pump just before all sample is gone. you should see a large plateau on the chromatogram.
v) Add approximately 10 mL buffer A at 5 mL/min to residual protein and run sample pump for <10 mL to ensure injection of all protein.
vi) Remove “His II peak fractions” falcon tube from the waste container. This is where your protein is.
vii) Switch sample pump flow selection to “Manual inject loop, system pump to column.” Flow line on computer diagram should show a red injection loop and a green line running from the system pump through the column and to waste.

4 Set up Fraction Collection

i) Ensure fraction collector is on, has clean racks in it, and is connected to the system
ii) Click on the blue fraction collector viewer icon and press both “Remove Empty Racks” and “Remove All”
iii) Close out window
iv) Double click on fraction collector to open window. Rack type should be F1 (12-13 mm X 100mm tubes). Start collection from A1 and end at B90. Fraction size should be 2 mL

5 Achieve Adequate Separation

i) Set system pump to 5 mL/min, 0% B, for 25 mL. Start Pump
ii) Turn on fraction collection by double clicking fraction collector and pressing “Collect.”
iii) Absorbance line should be near or at baseline after 25 mL run. If not, run 10 mL at a time until the baseline of A280 is less than 100 mAU

6 Elute His-tag and TEV from the column

iv) Under the system pump, choose gradient, initial %B 0%, final %B 100%, 25 mL then click the check box to run final B% for an additional 15 mL
v) Start flow. A peak should appear around 30%B

vi) At 100%B, you will notice that A280 flattens out around 500 mAU. To establish this is absorbance from the high concentration imidazole, run 15 mL 0%B and watch the absorbance line and the connectivity line. the line shapes should be very similar. A280 should drop down close to zero

7 Finishing up

i) Stop collection
ii) Press “Reset Arm”
iii) Save run: [protein_media_labelling, if applicable_date_initials]
iv) Close out run and open ‘Analysis’
v) Deselect every line trace except A280, A255, %B, and Connectivity
vi) Create run report under File
vii) Save in a folder created on desktop

SIZE EXCLUSION CHROMATOGRAPHY (SEC) PURIFICATION

The purpose of this step is to ensure that the protein collected from the previous purification steps is pure, and is the molecular weight expected for T4L. This column is much more fragile than the IMAC columns**. Maximum flow through these columns is 0.5 mL/min. Minimum volume required to equilibrate column is 120 mL so plan accordingly. If the column is stored in ethanol, it will require 120 mL of water, then 120 mL of SEC buffer to equilibrate, taking about 6-8 hours.**

Required Materials.

NGC liquid chromatography system running ChromLab program

T4L SEC Buffer (see page 8) placed in Buffer selector 6A

HIS-II purified peak fraction concentrated to under 5 mL

1 – 50 mL falcon tube labeled SEC purified T4L

Methods.

1 Ensure SEC column (column selector 5) is equilibrated to T4L SEC Buffer (Buffer selector 6) and baseline is zeroed

2 Direct inject the HIS-II purified, concentrated T4L onto the SEC column at 0.5 mL/min

3 Change the sample pump flow selector to "system pump to column, sample pump direct inject"

4 Set system pump for 0%B 120 mL at 0.5 mL/min and start the pump

5 Immediately start fraction collection (2 mL)

6 T4L will come off the column around 80 mL

7 Pool the peak fractions into the 50 mL falcon tube labeled "SEC purified T4L" and store in deli-style refrigerator.

8 Save run

APPENDIX C

Standard Operating Procedure (SOP): 2-ethynylpyridine (2-EP) kinetics assay

I. Principle of Concept

In laboratory science, assays are analytical techniques used for the qualitative assessment or quantitative measurement of a target entity[1]; from such, inferences can be made to either affirm hypotheses or supply conclusive evidence. This assay assesses the production of a conjugated polymer in the presence of lysozymes, a mechanism deviating from their native function. Over time, as product accumulates, a deep-red hue is elicited (visible to the naked eye); in monitoring this via hour reads, rate kinetics as well as concentration thresholds can be determined.

II. Resources

Materials/Reagents	Manufacturer	CAS/Catalog No.	Amount Needed*
2-ethynylpyridine, 97 %	Accela *via Fisher Scientific*	1945-84-2 / 50-648-599	*
96-well plate, clear	Costar *via Fisher Scientific*	07-200-95	1
Roche 480 sealing foil	LifeScience Roche	04 7297570 01	1
Purified, lysozyme strain:			
Bacteriophage T4	---	---	*
IVY class *c, p1, (p2?)*	---	---	*
Lysozyme, hen egg-white	Hampton Research	12650-88-3 / HR7-110	*
Nuclease-free water	IDT	11-05-01-04	*

*Amount is based on either stock or desired concentration; use molarity calculator to calculate values and q.s. with water. https://www.graphpad.com/quickcalcs/molarityform/

III. 2-ethynylpyridine (2-EP) kinetics assay protocol

Step 0. Open a Word document and format a table to emulate the 96-well plate; from left to right, the concentration of 2-EP varies while the concentration of lysozyme varies from top to bottom (see figure below). The first row will utilize HEWL (Hen Egg White Lysozyme) + 2-EP and act as a positive control to the experimental lysozyme. Likewise, a blank (consisting of water + 2-EP) is needed for each experimental well— this will act as the negative control.

[2-EP]

2-EP / T4L	60 mM 1.5uL	60 mM 1.5uL	90 mM 2.25uL	90 mM 2.25uL	100 mM 2.5uL	100 mM 2.5uL	120 mM 3.0uL	120 mM 3.0uL	150 mM 3.75uL	150 mM 3.75uL	180 mM 4.5uL	180 mM 4.5uL
0.0mM T4L (HEWL)	5.6 H 217.9	---------- 223.5	5.6 H 217.15	---------- 222.75	5.6 H 216.9	---------- 222.5	5.6 H 216.4	------ 222	5.6 H 215.65	------ 221.25	5.6 H 214.9	------ 220.50
0.125 mM T4L	36.24 T 187.26	------ 223.5	36.24 T 186.51	---------- 222.75	36.24 T 186.26	---------- 222.5	36.24 T 185.76	------ 222	36.24 T 185.01	------ 221.25	36.24 T 184.26	------ 220.50
[lysozyme]												

[1] *The American heritage dictionary of the English language (4th ed.). Boston, MA: Houghton Mifflin. 2006.*

Values of each reagent must be calculated and admixed in 1.7 mL Eppendorf centrifuge tubes prior to adding each reaction to the plate. Use GraphPad Molarity Calculator to ensure the accuracy of all calculations. https://www.graphpad.com/quickcalcs/molarityform/

For example, if the desired concentration of a reaction needed to be 125 µM lysozyme to 100 mM 2-EP in a final volume of 225 µL, given a stock concentration of lysozyme at 929 µM and the manufacturer concentration of 2-EP at 9 M, the calculation would be as follows:

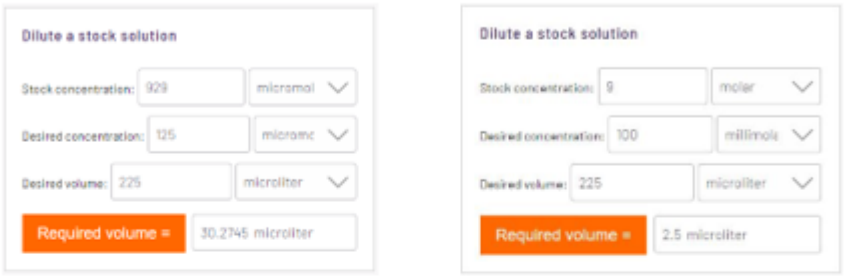

Both values are subtracted from the total volume of 225 µL thus giving the amount of nuclease-free water needed to receive the desired reaction values; in this case, 192.23 µL of water would be added to 30.27 µL of lysozyme* and 2.5 µL of 2-EP. *As 30.2745 µL cannot be pipetted accurately, the value is rounded down to 30.27 µL.

Step 1. Begin by gently vortexing each solution to ensure homogeneity. Using a P-1000 pipettor, pipet 200 µL of each solution into their respective wells. Be sure not to agitate the plate as spillover of one solution may contaminate the surrounding reactions.

Step 2. Apply a Roche 480 sealing foil to the 96-well plate to prevent evaporation or possible contamination of each reaction. **NOTE.** As these films are relatively expensive, if the range of experimental wells does not span the entirety of the plate, cut the sealing film as needed.

Step 3. Using a SpectraMax iD5 Microplate Reader, equipped with SoftMax Pro 7 or higher software, insert the 96-well plate into the designated area and close the system. The plate reader parameters are as follows; additional step-by-step visualization and information can be found in the appendix below:

Kinetic assay parameters. Spectrum absorbance: wavelengths ranging 300 nm to 600 nm, at 2 nm step increments. Temperature: 22 °C. Plate type: 96-well standard, clear bottom. Read area: [selected well area that will be analyzed]. Shake: 3 seconds, medium, orbital.

Organizational parameters. Each reaction should contain a blank, control well paired with the experimental well. To differentiate, coordinate each set with a unique color using the acquisition settings. The plate should resemble below.

Step 4. Upon completion, highlight all experimental wells, right-click the plate image and select 'copy plate data'. Paste the values into a new, google spreadsheet located on the **RIBONAUTS** drive. (see T. Leeper for username and password) Continue using this spreadsheet for all data compilation and organization for the current experiment. For data analysis/manipulation and visual representation, use GraphPad Prism software for "publication-ready" figures.